RESEARCH MEMORANDUM

PERFORMANCE AT MACH NUMBERS 3.07, 1.89, AND 0 OF INLETS DESIGNED FOR INLET-ENGINE MATCHING UP TO MACH 3

By L. W. Gertsma and M. A. Beheim

Lewis Flight Propulsion Laboratory
Cleveland, Ohio

NATIONAL ADVISORY COMMITTEE
FOR AERONAUTICS

WASHINGTON
May 20, 1958

NATIONAL ADVISORY COMMITTEE FOR AERONAUTICS

RESEARCH MEMORANDUM

PERFORMANCE AT MACH NUMBERS 3.07, 1.89, AND 0 OF INLETS DESIGNED FOR INLET-ENGINE MATCHING UP TO MACH 3

By L. W. Gertsma and M. A. Beheim

SUMMARY

The performance of a two-dimensional external-compression inlet designed for various methods of inlet-engine matching up to Mach 3 was investigated at Mach 1.89 and Mach 0. Angle-of-attack data at Mach 3.07 were also obtained.

Supersonic spillage by rotating the ramp as a unit gave higher critical pressure recoveries and smaller distortions than any other matching method investigated for the two-shock and, at the lower mass flows, for the isentropic inlets. The throat bypass had the best performance of the bypasses with both ramps and especially with the isentropic ramp at mass-flow ratios near 80 percent. All configurations were stable over a range of mass flow of 10 percent or better at zero angle of attack.

When the top bypass was used as an auxiliary inlet at Mach 0 with the flow divider rotated into the free-stream, pressure recovery increased and distortion decreased. With the flow divider out and only the top door open, the increase in recovery was not as large and distortion was increased.

INTRODUCTION

As design Mach number increases, aircraft having air-breathing engines must have larger air inlets in order to supply the necessary air to the engines. These inlets should be variable-geometry types in order to give good performance at lower Mach numbers. Since, in general, a variable-geometry inlet designed for high Mach numbers usually will capture more air than the engine can use at lower Mach numbers, the excess must either be spilled ahead of the inlet or bypassed around the engine. These operations must be accomplished efficiently to keep the drag at a minimum.

An investigation has been conducted at the NACA Lewis laboratory to determine the performance of an inlet, designed for Mach 3, when operated

at Mach 1.89 with different bypass and spillage arrangements. No attempt was made to match this inlet to any particular engine; therefore, no match lines are shown on the figures. The model design made it possible to operate the inlet at critical conditions over a very wide range of mass-flow ratios. This inlet was also investigated at Mach 0 to determine the performance at takeoff both with and without one of the bypasses arranged as an auxiliary inlet. The zero-angle-of-attack performance of this inlet at Mach 3.07 is reported in reference 1.

SYMBOLS

$C_{D,c,p}$ cowl drag coefficient from measured pressures

m mass flow

P total pressure

Subscripts:

0 conditions in free stream in capture area of inlet

1 inlet throat

3 compressor face

Superscript:

* choked flow under ideal conditions

APPARATUS AND PROCEDURE

MODEL

The investigation was conducted on a two-dimensional model designed for inlet-engine matching up to Mach 3. Photographs and sketches of the model appear in figure 1, where the nomenclature used in referring to the various parts of the diffuser is indicated. The model was mounted in the tunnel with the compression surface on the lower side of the inlet. Either a two-oblique-shock or isentropic ramp could be used. The two-shock surface was hinged between the ramps and could be pivoted about the leading edge so that any angle could be set on either ramp. The center section of the isentropic ramp was made of spring steel; and, by adjusting the rear rigid section and pivoting the ramp about the leading edge, a variety of contours could be obtained.

Matching methods illustrated in figure 1 are (1) supersonic spillage by rotating the ramps, (2) top bypass with flow divider and control

door, (3) top bypass without flow divider, (4) throat bypass with bottom control door, and (5) bottom bypass and control door with short diffuser plate. Any of these matching methods could be used with either compression surface. The ram scoop used for the throat bypass could also be used for boundary-layer bleed with the other matching methods.

Internal area variations of the diffuser are shown in figure 2 for typical positions of both ramps at Mach 1.89. The basic diffuser (bypass not used) had a fairly continuous area variation at these off-design conditions; but, when the flow divider was removed for a top bypass configuration or when the short diffuser plate was used for the bottom bypass arrangement, an overexpansion and an abrupt contraction occurred.

The various contours of the isentropic ramp that were used are shown in figure 3. The Mach 3.07 contour was the design contour at Mach 3.07 and was rotated as a unit to several angular positions in the present test. In the absence of the external cowl shock, the Mach 1.89 contours, which were obtained by flexing the ramp from an initial angle of either 0° or 6°, would have focused the compression waves at the cowl lip at a free-stream Mach number of 1.89.

The cowl was designed with an initial external angle of 31°, but during construction the leading edge was bent to 39° (fig. 3). This difference did not change the location of the leading edge. Since both the actual and the theoretical external cowl angles exceeded the shock-detachment value of 21° for Mach 1.89, this difference was not considered important to the diffuser internal performance.

DATA REDUCTION

Mass-flow ratios were calculated using the method of a choked exit plug and the average total pressure at the plug (which was obtained from a 40-tube rake in front of the plug) and a flow coefficient of 0.965. This value of flow coefficient was obtained in an earlier test at Mach 3.07 where the capture mass-flow ratio was known to be 1.0. Total-pressure recovery and distortion were obtained from an 18-tube rake arranged for area-weighted averages about a simulated compressor hub. A static-pressure pickup was attached at the compressor station. The total-pressure profiles at the throat were measured just behind the cowl-lip plane. The reference mass flow for Mach 0 was computed assuming an ideal inlet and diffuser and choked flow at the compressor station.

Traces from the static-pressure pickup are shown in figure 4 for different types of inlet operation. Flutter is used to define a local oscillation of the normal shock during subcritical operation, and buzz refers to a violent oscillation of the normal shock out to the front of the ramp. Actual pressure values taken from the traces are not considered accurate because of inertia in the recorder.

TUNNEL

The Mach 1.89 investigation was conducted in the Lewis 18- by 18-inch tunnel. The total temperature was 150° F, and a dewpoint less than 0° F was maintained. Tunnel calibrations show that the total pressure at the test section is 0.972 of that upstream of the nozzle. This value was used in the calculations, but some inlet throat total-pressure recoveries obtained late in the test were as much as 2 percent greater than unity. Therefore, the correct value of free-stream total pressure is somewhat in doubt, and there is a possibility that recoveries reported here may be as much as 2 percent too high. An error of this size would cause less than a 1-percent increase in mass-flow ratio.

The Mach 3.07 investigation was conducted in the same facility as used in reference 1.

The Mach 0 investigation was conducted in the Lewis duct tunnel. The model was installed with the inlet open to the atmosphere and the exit connected to exhausters through a surge tank.

RESULTS AND DISCUSSION

INLET PERFORMANCE AT MACH 1.89

Shock Geometry

The non-internal-contraction design selected for the inlet employed a high external cowl-lip angle that exceeded the shock-detachment angle of 21° at the test Mach number of 1.89. Schlieren photographs in figure 5 show the location of the shocks for the two-shock and the isentropic ramps during critical operation at Mach 1.89. In these photographs the terminal angle of the two-shock ramp was near detachment and the terminal angle of the isentropic was near the theoretical angle required to turn the flow to Mach 1.

Two-Shock Ramps

Effect of ramp angles. - The inlet performance with various two-shock ramp positions is shown in figure 6. By rotating the Mach 3.07 design setting of 15° and 30° as a unit about the first-ramp leading edge until the second shock would theoretically fall on the lip, neglecting the presence of the detached cowl shock, ramp angles of $5\frac{3^\circ}{4}$ and $20\frac{3^\circ}{4}$ are

obtained. When the two-shock ramp was rotated as a unit to higher angles, critical pressure recovery increased and distortion decreased. The decrease in distortion was partly a result of the decrease in compressor-face Mach number as mass flow decreased. For these data, the throat ram scoop was maintained at a constant 1/8-inch height for all ramp positions. This height was near optimum at the design Mach number of 3.07 (ref. 1).

Effect of bypass. - All bypasses were investigated with the $5\frac{3^\circ}{4}$ and $20\frac{3^\circ}{4}$ ramp angles, and the results are shown in figure 7. Figure 7(a) shows that both the critical recovery and distortion decreased slightly as the throat scoop height was increased. Subcritical recovery increased when the ratio of scoop to throat height was 0.375 or larger. For the data with the other bypasses in figure 7, the ram-scoop height was maintained at 1/8 inch. When the top bypass was used (fig. 7(b)), critical recovery and distortion decreased slightly with increased amounts of bypass bleed. Without the flow divider (fig. 7(c)), both the critical recovery and distortion remained constant as bleed increased. Bleed through the bottom bypass (fig. 7(d)) increased distortion but had little effect on recovery. In this case discontinuities occurred during supercritical operation with large amounts of bypass bleed.

Critical performance. - A summary of the critical performance from the preceding curves, shown in figure 8, indicates higher recovery and lower distortion with either higher ramp angles or with boundary-layer bleed, or both. When the ramps were rotated independently to the theoretically optimum angles for pressure recovery (fig. 8(a)), critical pressure recovery was higher at a given mass-flow ratio than when the ramps were rotated as a unit.

A comparison of spillage methods (fig. 8(b)) shows that rotating the ramps as a unit for shock spillage gave the highest critical recovery and lowest distortion. Of the bypasses, generally, the throat bypass had the highest recovery and the lowest distortion at any given mass flow. The bottom bypass had the poorest performance primarily because of the high distortion.

Isentropic Ramp

Effect of ramp setting. - The inlet performance with a variety of isentropic ramp contours and a constant ram-scoop height of 3/16 inch, which was near optimum at Mach 3.07, is shown in figure 9. When the Mach 3.07 contour was rotated about the leading edge for supersonic spill, the recovery increased and the distortion decreased at the higher ramp angles. All ramp settings tended to have a wide stable range. The subcritical recovery of the higher ramp angles was very high. The distortions were

more a function of mass flow than of ramp settings or contours. As the ramp angles increased, the strength of the detached cowl shock decreased, which could have some effect on the operating characteristics of the inlet.

Effect of bypass. - The performance of the various bypass systems with the Mach 3.07 ramp contour (0° and 22.4°) is shown in figure 10. Small amounts of throat bleed (fig. 10(a)) increased the critical recovery, but as the bleed was increased further the critical recovery decreased. Subcritical stability remained large with about the same recovery for all scoop heights.

For the other bypass data in the figure, the ram-scoop height was maintained at 3/16 inch. Critical recovery decreased as much as 5 percent as bleed was increased through the top bypass with the flow divider (fig. 10(b)), but the subcritical recovery remained about the same, with a large stable range. Critical distortion remained high as bleed was increased.

Bleed through the top bypass without the flow divider increased subcritical recovery slightly, but critical recovery stayed about the same (fig. 10(c)). Increased bleed aggravated distortion. Removing the divider did not produce any appreciable improvement in distortion, whereas it did at Mach 3 (ref. 1). This can partly be attributed to the fact that the percentage area discontinuity caused by removing the divider was not as large with the Mach 1.89 ramp position as with the Mach 3.07 positions.

Small amounts of bleed through the bottom bypass increased critical recovery, but recovery then decreased for large amounts of bleed (fig. 10(d)). Subcritical recovery was about constant, and the stable range was a little larger than for the other bypasses. Distortion remained high even at low mass flows.

The bypass performance with the Mach 1.89 contour (0° and 22.4° ramp angles) is presented in figure 11. The effect of throat bleed (fig. 11 (a)) was about the same as for the Mach 3.07 contour. Low bleed rates increased critical recovery slightly, but higher bleed rates decreased it. Subcritical recovery peaked and then decreased as mass flow was reduced, but the stable range remained quite large. Distortion again was nearly a function of mass flow, decreasing as the mass flow decreased.

For the remaining bypass data in this figure, a constant ram-scoop height of 3/16 inch was used. When the top bypass was used both with and without the flow divider, critical pressure recovery increased slightly with small amounts of bypass bleed (figs. 11(b) and (c)). With the flow divider, there was a small stable range that peaked just before buzz. The stable range was about twice as large without the divider as with it. Distortions were nearly constant for all bypass bleeds with the divider but varied with the mass flow without the divider.

[redacted]

There were erratic supercritical mass-flow changes when the bottom bypass with the short diffuser plate was used (fig. 11(d)). These variations probably were a result of the particular position of the normal shock with respect to the bypass. All pressure recoveries decreased with high bypass bleed; and the distortion, which was high with no bleed, became worse as the bleed was increased.

The Mach 1.89 contour (6° and 21.2°) was investigated only with the throat bypass (fig. 12). The recovery increased and then decreased as the bleed rate was increased, while the distortion decreased steadily.

Critical performance. - A summary of critical operation with the various isentropic ramp contours (fig. 13(a)) shows that small amounts of bleed through the ram scoop increased critical recovery and lowered distortion for all contours. Rotating the Mach 3.07 contour ramp as a unit to higher angles increased recovery until the shock detached from the rear of the ramp, and then the recovery decreased. The difference between the Mach 3.07 contour and the Mach 1.89 contour at approximately the same final ramp angle is probably a result of the change in cowl shock strength as the contour of the ramp and the attendant compression zone are changed.

The critical recovery increased with throat bleed (fig. 13(b)) to a maximum for each contour and then dropped off as the bleed was further increased. For most of the contours, as throat bleed was increased, the distortion decreased. This was partly due to the lower Mach number at the compressor.

Comparison of the different matching methods at critical operation with the Mach 3.07 contour shows that the highest recovery and the lowest distortion were obtained at high mass-flow ratios with the throat bypass and at low mass-flow ratios with supercritical spillage by the ramp (fig. 14(a)). The top bypass without flow divider was the least effective with the Mach 3 contour. All methods with the Mach 1.89 contour were nearly the same for critical recovery and distortion with the exception of the bottom bypass, which had large distortions at low mass flows (fig. 14(b)).

Profiles

Critical pressure-recovery contours at the compressor face are shown in figure 15 to compare the effect of the different bypasses on the distortion. All the contours are symmetrical about a vertical line through the hub with an area of high pressure next to the hub on each side. Using bypasses on either the top or bottom of the diffuser shifted these high-pressure regions toward the bypass.

Pressure-recovery profiles at the throat during critical operation for the two-shock and isentropic ramps were nearly uniform for the high ramp angles but were poor for some of the lower ones (fig. 16). With the low ramp angles, the effect of the detached cowl shock would become more evident. Some of the recovery ratios with the isentropic ramp exceeded unity, indicating, as noted earlier in the APPARATUS AND PROCEDURE section, that the calibration of tunnel total pressure was low for this investigation.

Cowl Drag

The measured cowl pressure-drag coefficients decreased with decreasing mass flow (fig. 17). The coefficients did not vary by much more than 0.03 at any given mass-flow ratio for the various two-shock ramp positions (fig. 17(a)), but the variation was greater with the isentropic ramp positions (fig. 17(b)).

INLET PERFORMANCE AT ANGLE OF ATTACK

Mach 3.07

The model was also investigated through a range of angle of attack and yaw. The two-shock ramp (15° and 30°) at Mach 3.07 with throat bleed had a critical recovery varying from 53 to 67 percent for angles of attack of $+8^\circ$ to -8° and angles of yaw up to 7° (fig. 18). The stability range was very small for positive angles of attack but improved for the negative angles. Distortion was nearly the same for all angles, except for the 7° yaw, where it was much worse.

The isentropic Mach 3.07 contour (6° and 28.4°) with throat bleed had critical recoveries that ranged from 49 to 75 percent for angles of attack of $+8^\circ$ to -8° and yaw angles up to 7° (fig. 19). The stability range was 35 percent at -8° angle of attack but dropped to 5 percent at $+8^\circ$. At angles of yaw there was no stable range.

Mach 1.89

Critical pressure recovery of the two-shock ramp $\left(5\frac{3}{4}^\circ \text{ and } 20\frac{3}{4}^\circ\right)$ with throat bleed at Mach 1.89 varied between 74 and 92 percent for angles of attack from $+8^\circ$ to -8° and yaw up to 8° (fig. 20(a)). Stability range was fairly uniform at all angles. The trends in distortion were about the same for all angles except at 8° yaw, where there was a considerable increase at subcritical operation, which might be a result of separation on the side fairing.

[redacted]

Some typical bypass settings were investigated with the two-shock ramp at angles of attack and yaw. With throat bypass at a ratio of scoop to throat height of 0.250, the critical recovery at each angle of attack or yaw changed very little from that with no bypass, although the stable range did increase (fig. 20(b)). Distortions were the same as without a bypass, except that there was no increase at subcritical operation at angles of yaw.

The top bypass with flow divider at a ratio of divider to throat height of 0.250 and with throat bleed had a pressure recovery and stable range about the same as without a bypass, but the spread in mass flow was smaller for the same model attitudes (fig. 20(c)). Distortions were also about the same as without a bypass.

The critical recovery of the isentropic ramp with Mach 3.07 contour (0° and 22.4°) with throat bleed ranged from 78 to 94 percent for angles of attack from $+8^\circ$ to -8° and yaw angles up to 7° at Mach 1.89 (fig. 21). The stability range was 25 percent at 0°, -4°, and -8° but decreased to 5 percent for $+4^\circ$ and all angles of yaw. All distortions were near that for the zero attitude except at $+8^\circ$, when distortion was higher.

INLET PERFORMANCE AT MACH 0

Two-Shock Ramps

It may be mechanically feasible to use the top bypass as an auxiliary inlet to improve the Mach 0 performance. The flow divider could be rotated into the free stream, or if it were removed the top control door could be opened. The effect on performance with the two-shock ramp is shown in figure 22. In figure 22(a), the performance without the auxiliary inlet is shown with several ramp angles. The pressure recovery decreased and distortion increased as mass flow increased at all ramp settings. When using the two-shock ramp, the air choked at the compressor before it did at the inlet entrance. The ramp position 0° and 0° had the highest recovery and also nearly the highest distortion.

The inlet performance with the flow divider rotated into the free stream as an auxiliary inlet is shown in figure 22(b) for several positions of the divider and with the compression ramp set at 0° and 0°. Pressure recovery was increased appreciably and distortion was less than without the auxiliary inlet. Without the flow divider but using the top control door (fig. 22(c)), pressure recovery was not as high as with the flow divider but higher than without an auxiliary inlet. However, distortion was even higher than without the auxiliary inlet. The inlet performance with the flow divider rotated into the free stream for ramp angles of 0° and $7\frac{1}{2}^\circ$, and 0° and 15° is shown in figures 22(d) and (e), respectively.

Isentropic Ramp

In figure 23, the inlet performance with the Mach 3.07 contour (0° and 22.4°) is presented. Without an auxiliary inlet, the air could be choked at the diffuser entrance. The inlet performance using the flow divider as an auxiliary inlet appears in figure 23(a) and without the flow divider in figure 23(b). The top bypass with the flow divider again was a better auxiliary inlet than it was without the flow divider. Figures 24 and 25 show the inlet performance with the Mach 3.07 contour (-12.3° and 10.1°) and a flat wedge contour (6° and 6°), respectively, with the flow divider rotated into the free stream.

SUMMARY OF RESULTS

The performance of a two-dimensional, external-compression inlet designed for efficient engine-inlet matching up to Mach 3 was investigated at Mach 1.89 and Mach 0. The inlet could be operated with either a variable two-oblique-shock or a variable isentropic-compression surface. For matching, air could be bypassed through doors on opposite sides of the subsonic diffuser or through a ram scoop in the throat, or the compression surface could be rotated to give supersonic spillage. At Mach 0, the bypass opposite the external compression side could be opened for use as an auxiliary inlet. The following results were obtained:

1. Of all match methods with the two-shock ramp, supersonic spillage by rotating the ramps as a unit with a 15° included angle gave the highest critical pressure recovery and the least distortion over the complete range of mass flows.

2. With the two-shock $\left(5\frac{3}{4}^\circ \text{ and } 20\frac{3}{4}^\circ\right)$ ramp and bypasses, the highest recovery at all mass flows and the lowest distortion at the lower mass flows were obtained using a throat bypass, but stability for all configurations was about the same. Both the top bypass and the bottom bypass had about the same critical recovery. The bottom bypass had the highest distortion.

3. With the isentropic ramp, the Mach 3.07 contour rotated as a unit to match by supersonic spillage and the Mach 3.07 contour (0° and 22.4°) with throat bypass were the better matching methods at low and high mass flows, respectively. Best critical recovery was about 94.5 percent.

4. The pressure recoveries with the Mach 1.89 contours and the different bypasses were all below 90 percent, with distortions about the same or slightly lower than those for the Mach 3.07 contour.

[redacted]

5. Performance at angles of attack between -8° and $+8^{\circ}$ with the compression surface on the lower side showed good stability and recovery at negative angles of attack, both stability and recovery decreasing at positive angles.

6. When the top bypass was used as an auxiliary inlet at Mach 0 with the flow divider rotated out into the free stream, the pressure recovery increased appreciably. Without the flow divider, the increase in recovery was not as large.

7. The distortions generally decreased when the flow divider was used as the auxiliary inlet; but opening the top door without the flow divider resulted in distortions higher than those without an auxiliary inlet.

Lewis Flight Propulsion Laboratory
National Advisory Committee for Aeronautics
Cleveland, Ohio, February 20, 1958

REFERENCE

1. Beheim, M. A., and Gertsma, L. W.: Performance of Variable Two-Dimensional Inlet Designed for Engine-Inlet Matching. I - Performance at Design Mach Number of 3.07. NACA RM E56H23, 1956.

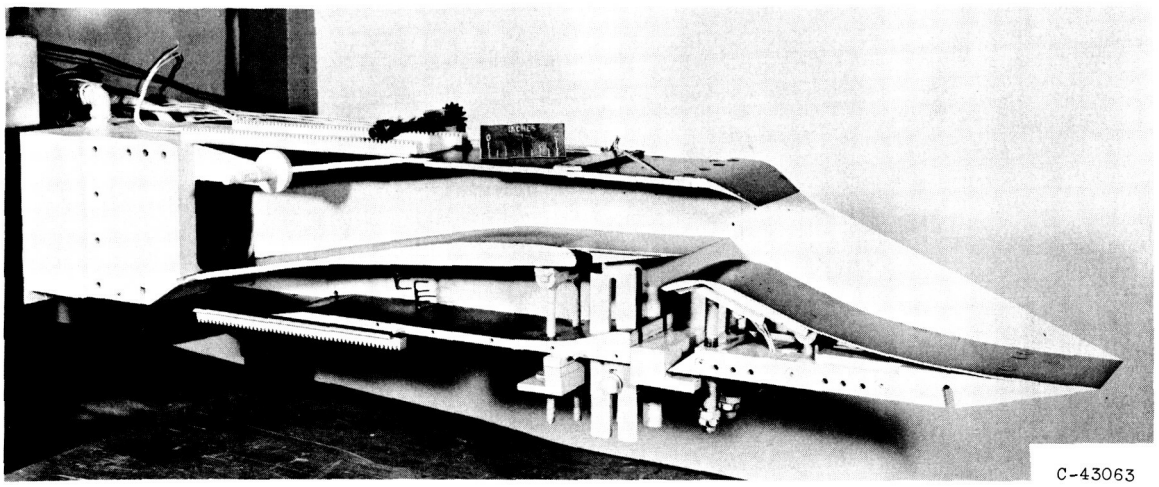

(a) Throat bypass arrangement.

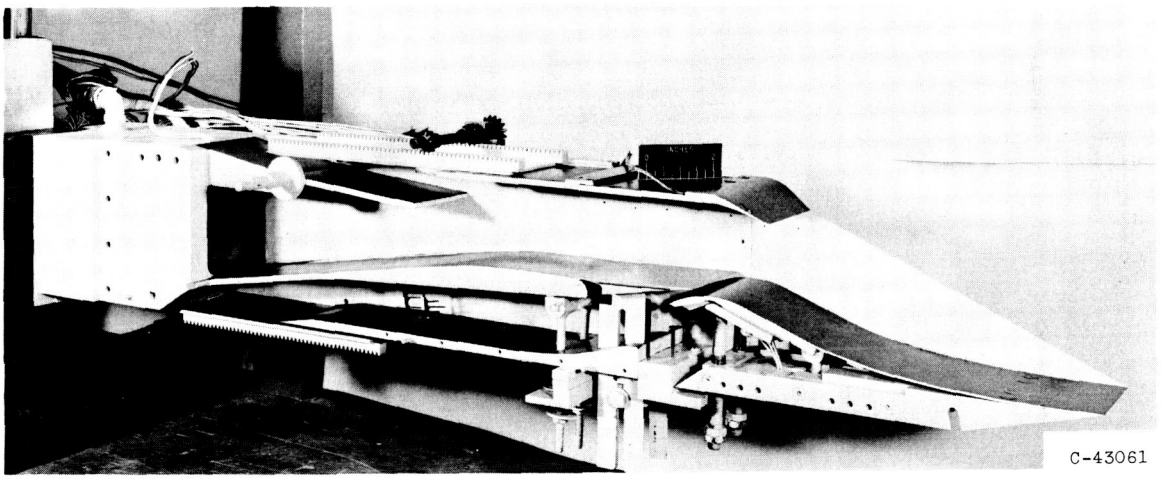

(b) Top bypass arrangement with flow divider and throat bleed.

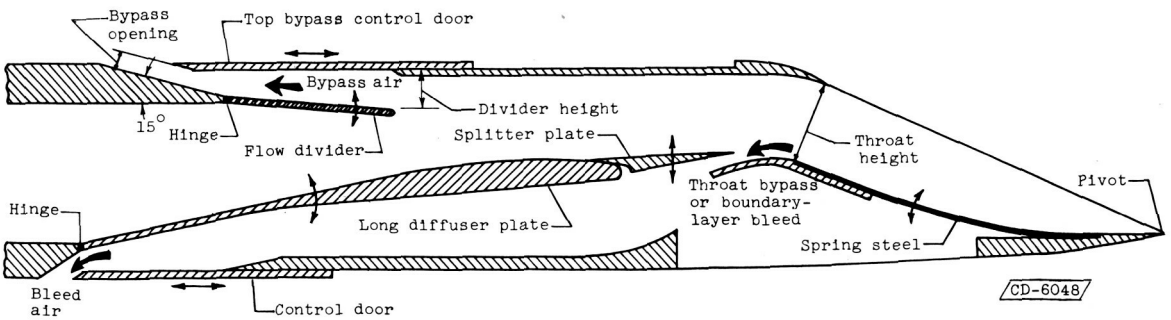

(c) Schematic view showing operation of throat and top bypass arrangement with isentropic ramp.

Figure 1. - Geometry of bypass arrangements.

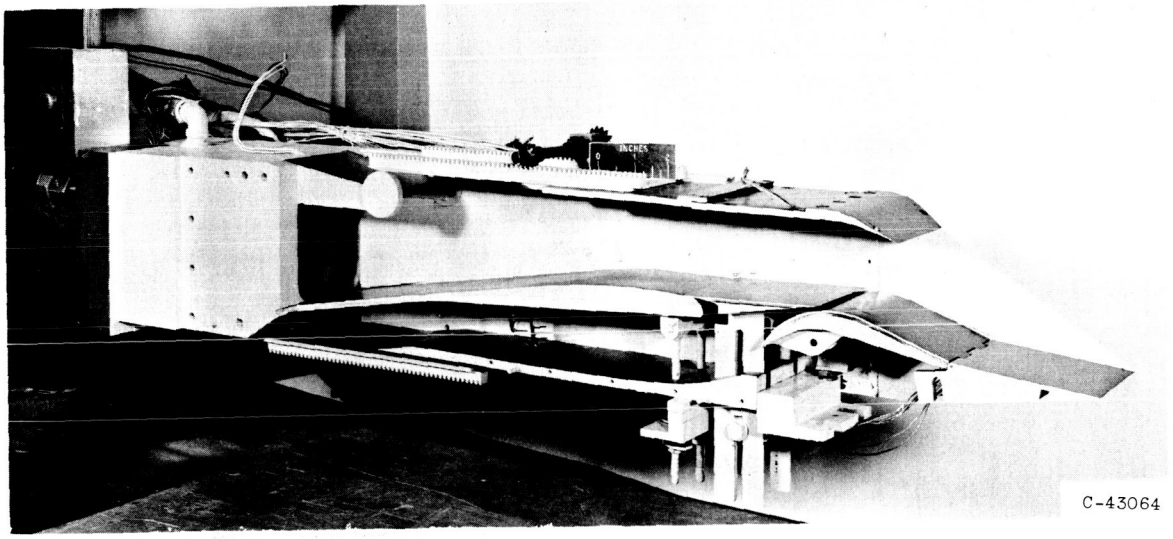

(d) Top bypass arrangement without flow divider and with throat bleed.

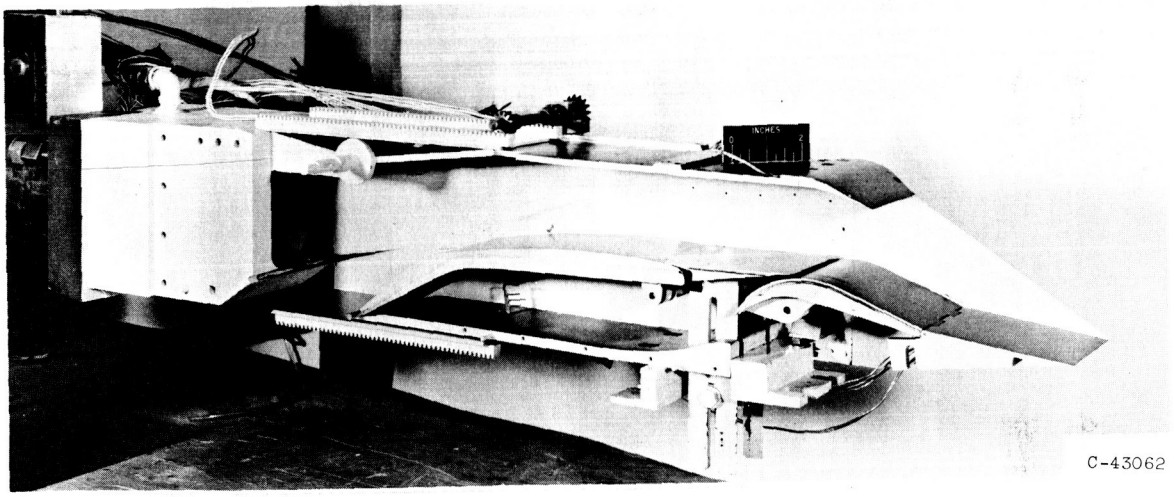

(e) Bottom bypass arrangement with throat bleed.

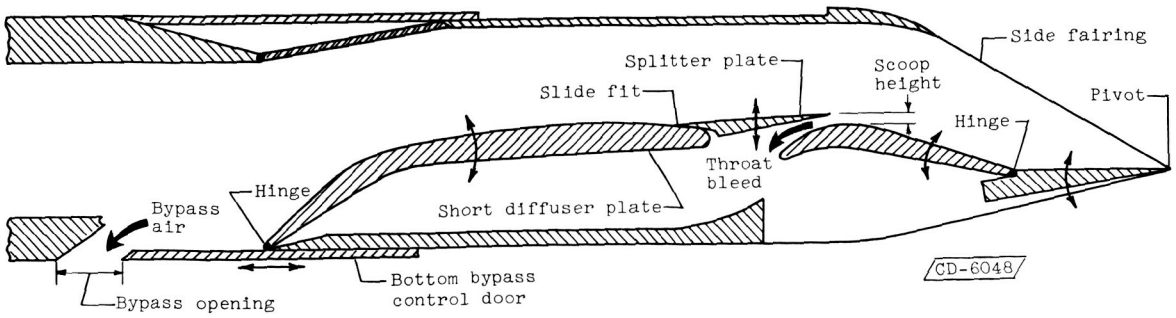

(f) Schematic view showing operation of bottom bypass with two-shock ramp.

Figure 1. - Concluded. Geometry of bypass arrangements.

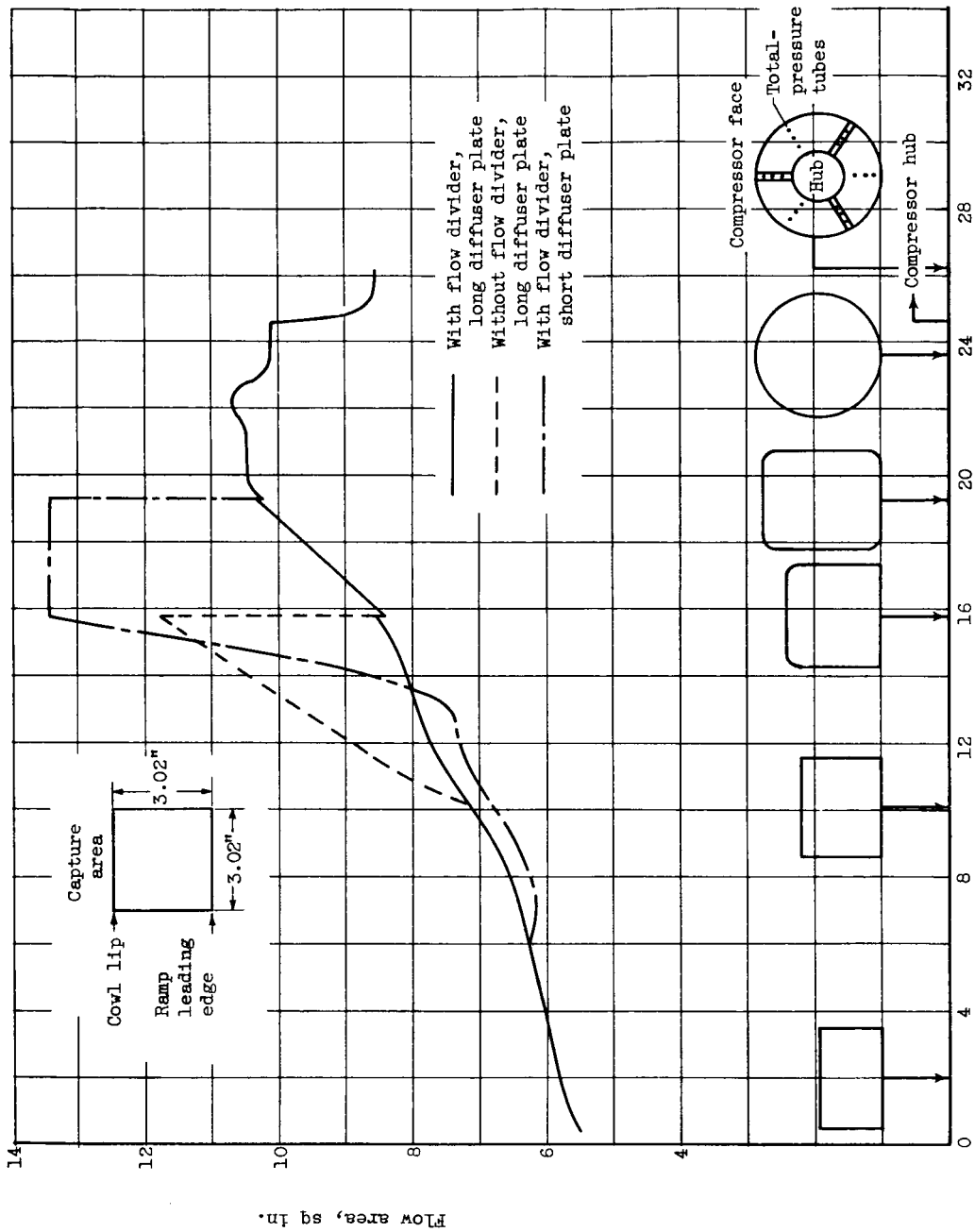

(a) Two-shock ramp. Ramp angles, $5\frac{3^\circ}{4}$ and $20\frac{3^\circ}{4}$; ratio of scoop to throat height, 0.

Figure 2. - Diffuser area variations.

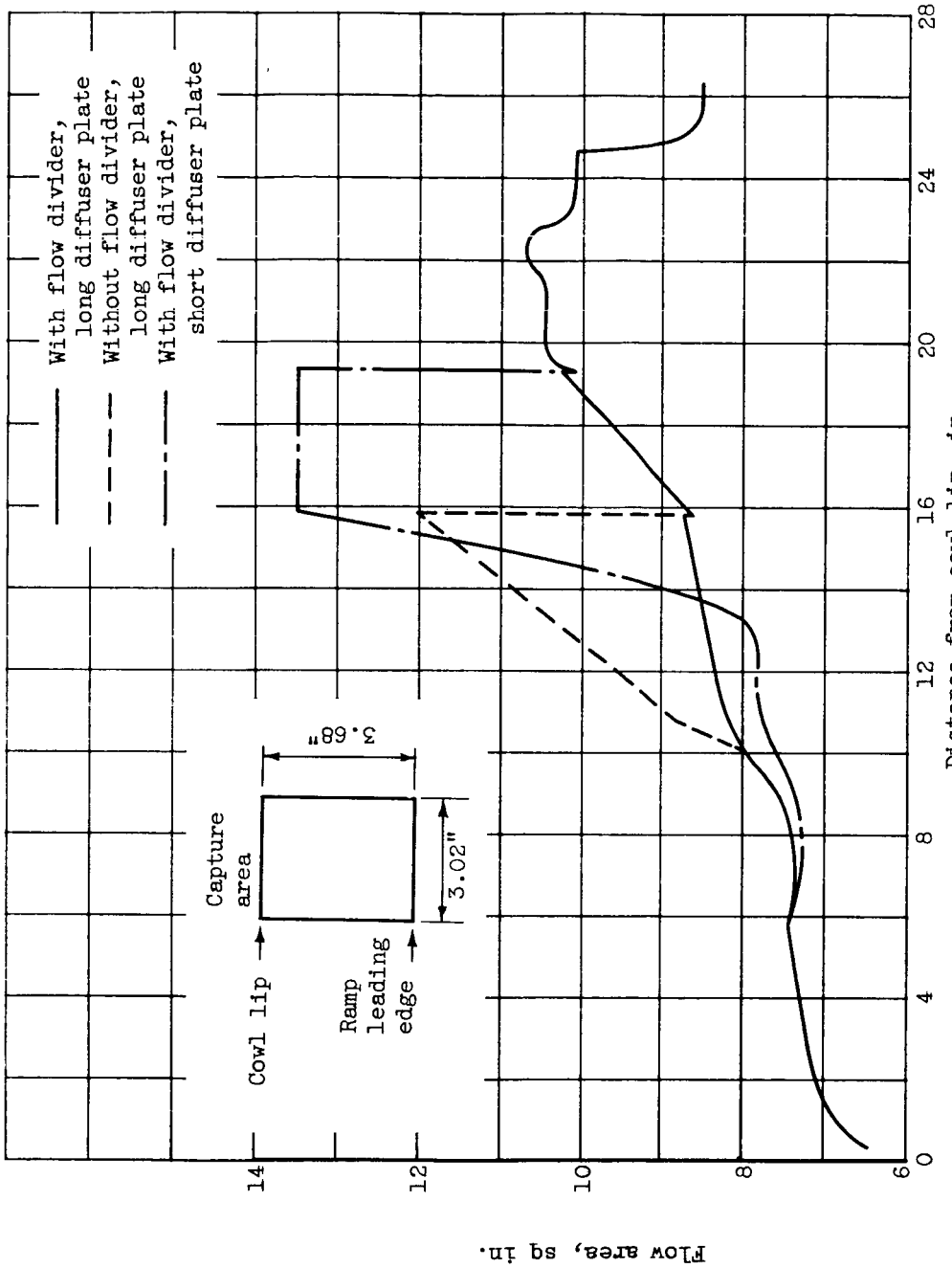

(b) Isentropic ramp with Mach 3.07 contour (0^{o} and 22.4^{o}). Ratio of scoop to throat height, 0.

Figure 2. - Concluded. Diffuser area variations.

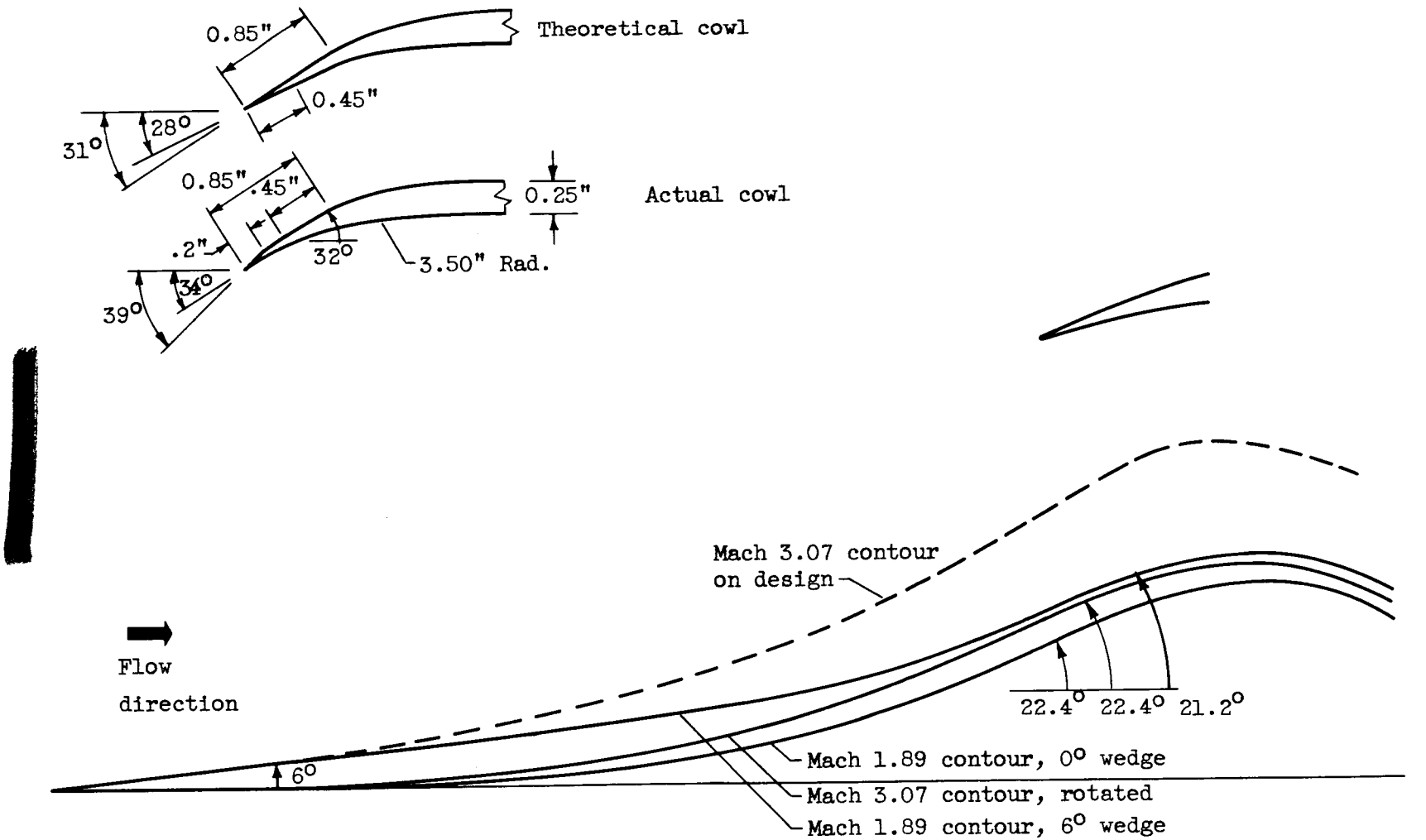

Figure 3. - Isentropic ramp contours (scaled).

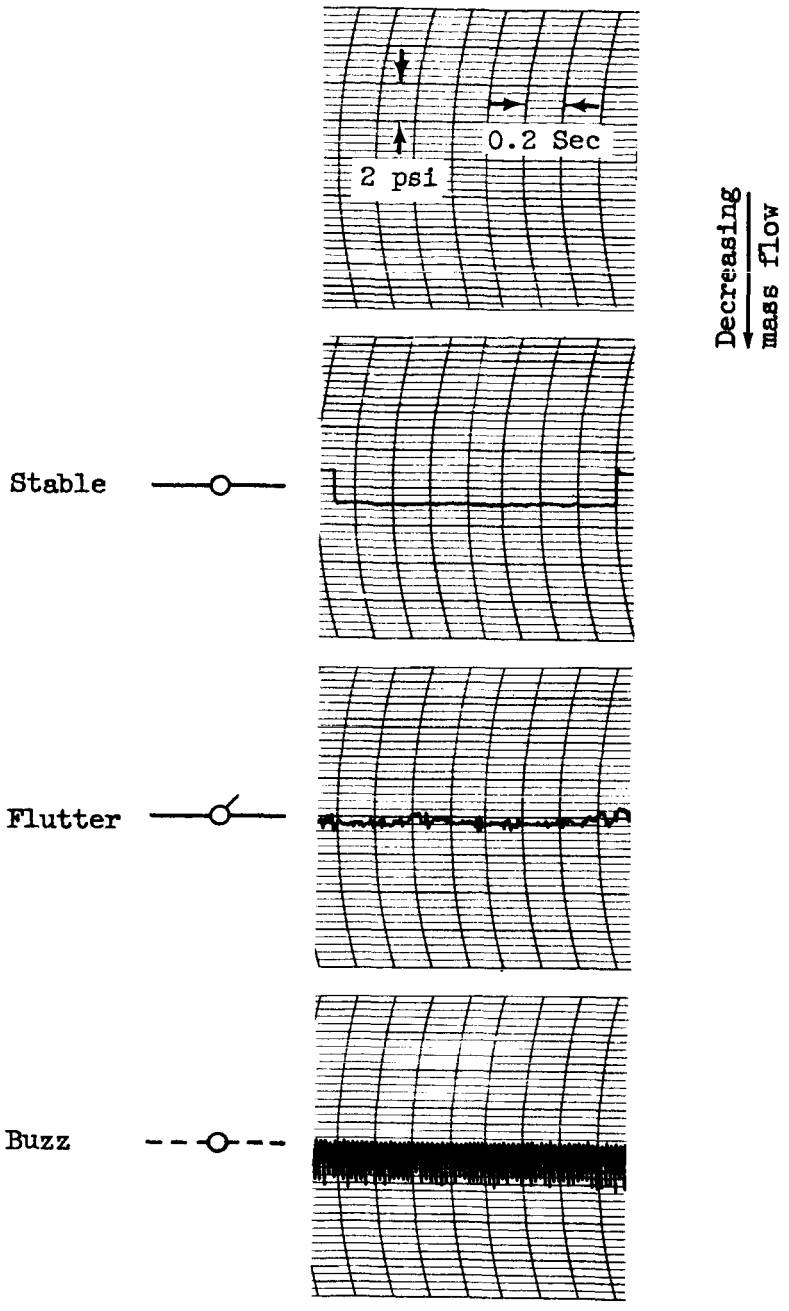

Figure 4. - Definition of inlet stability symbols for Mach 1.89.

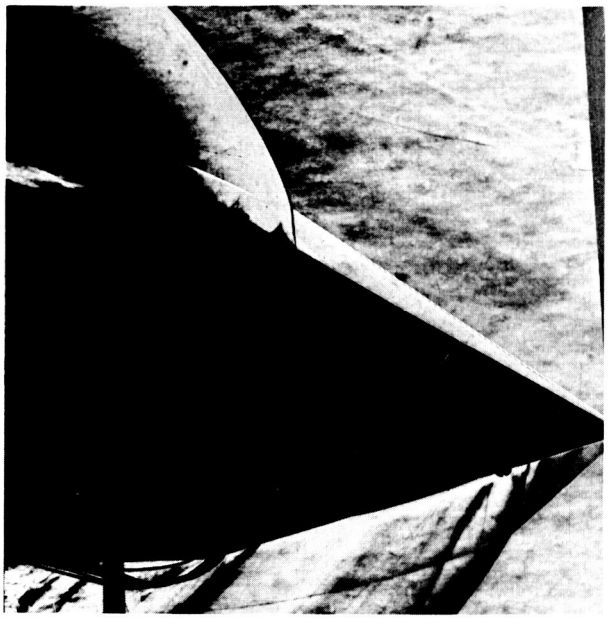

(a) Two-shock ramp, $5\frac{3}{4}^{\circ}$ and $20\frac{3}{4}^{\circ}$.

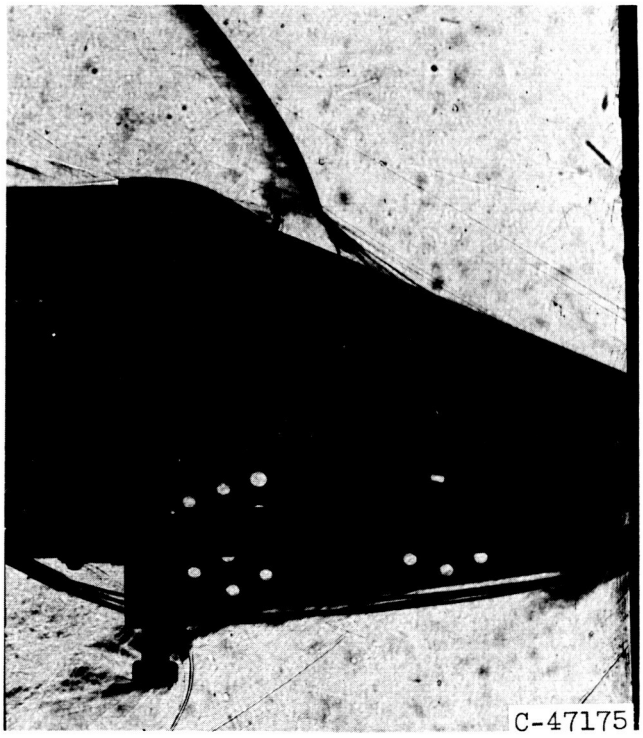

(b) Isentropic ramp, 0° and 22.3°.

Figure 5. - Schlieren photographs of model; critical operation at Mach 1.89.

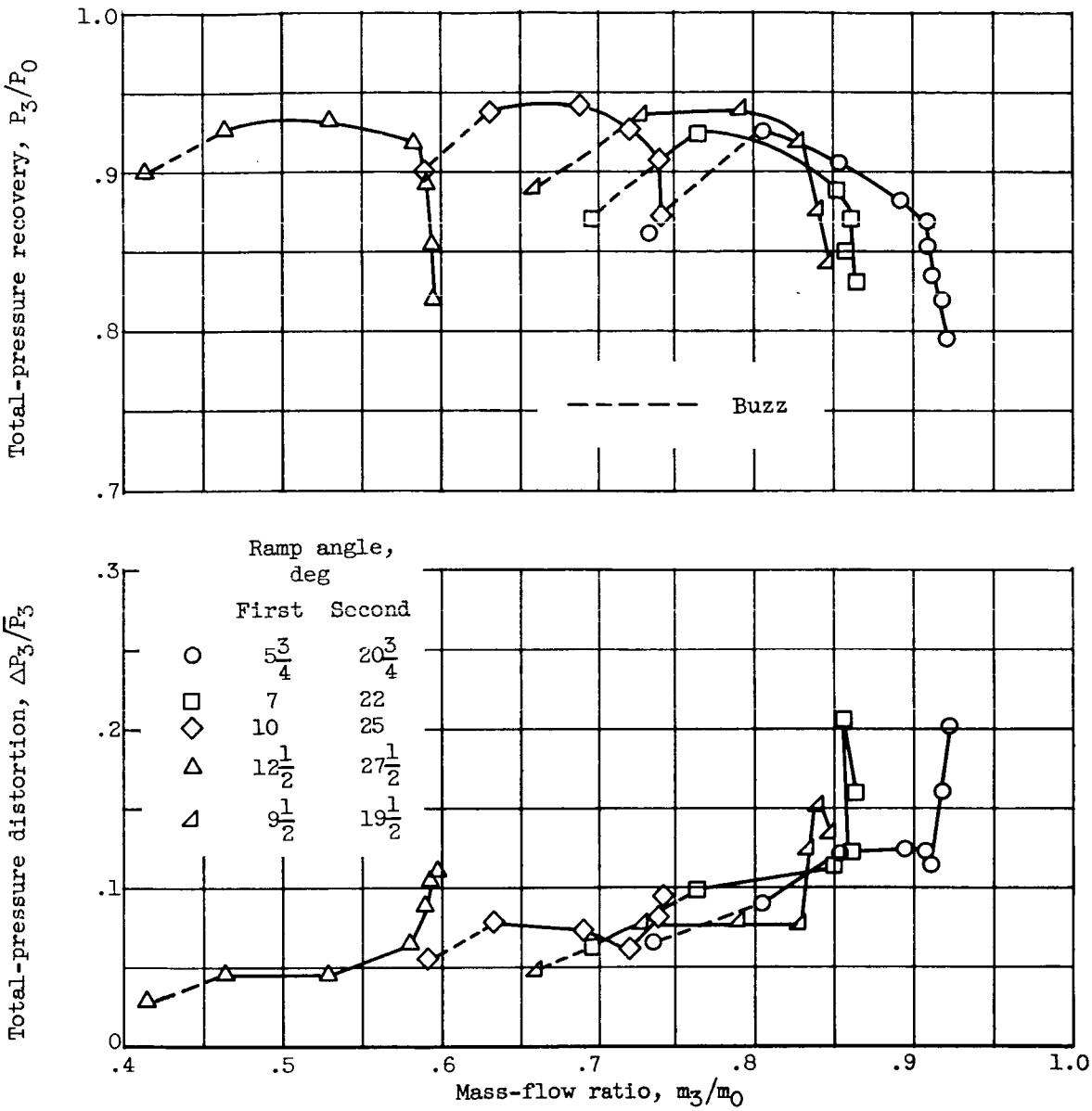

Figure 6. - Performance of two-shock ramp using different ramp angles with constant scoop height at Mach 1.89.

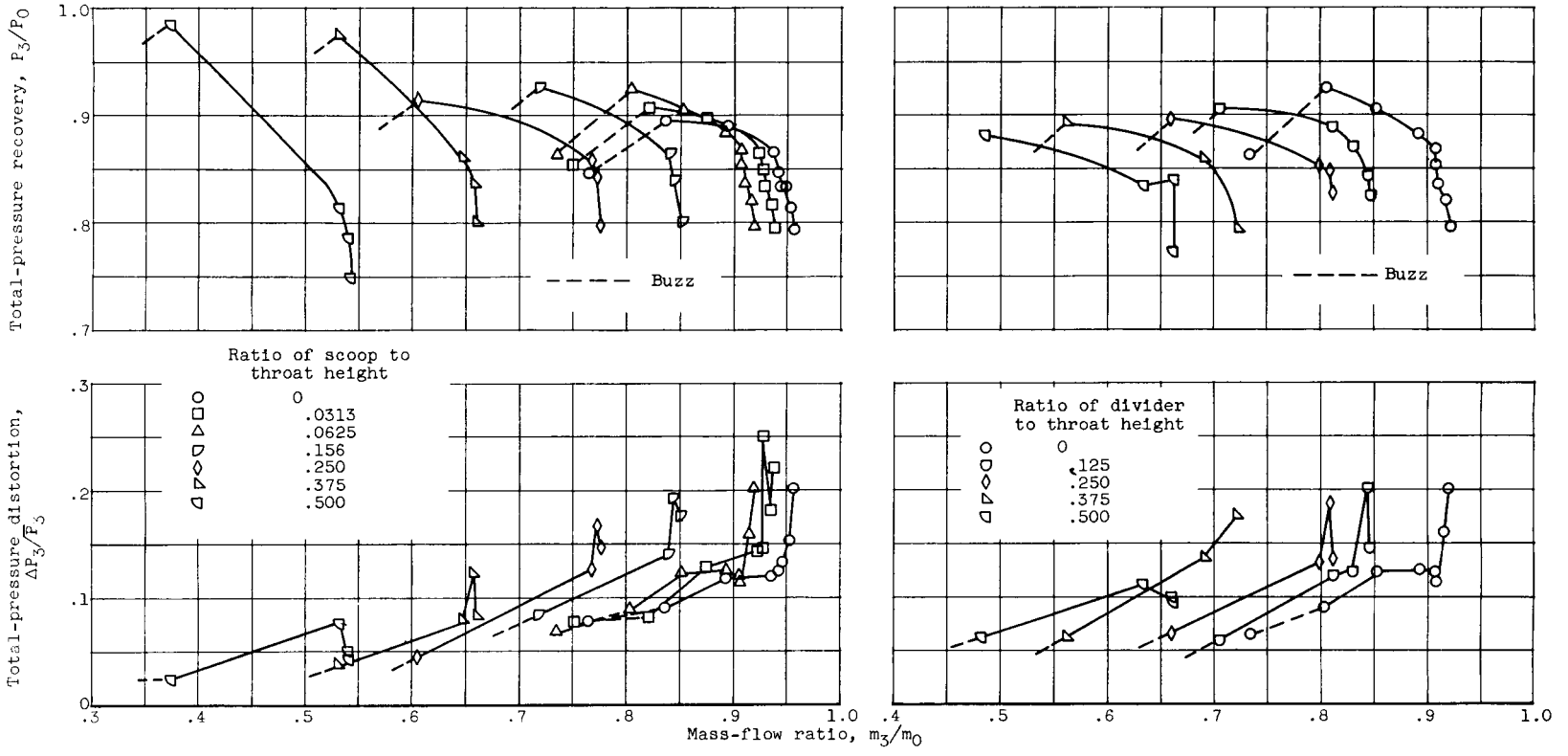

(a) Throat bypass.

(b) Top bypass with flow divider. Ratio of scoop to throat height, 0.065.

Figure 7. - Performance of two-shock ramp ($5\frac{3}{4}^\circ$ and $20\frac{3}{4}^\circ$) with different bypasses at Mach 1.89.

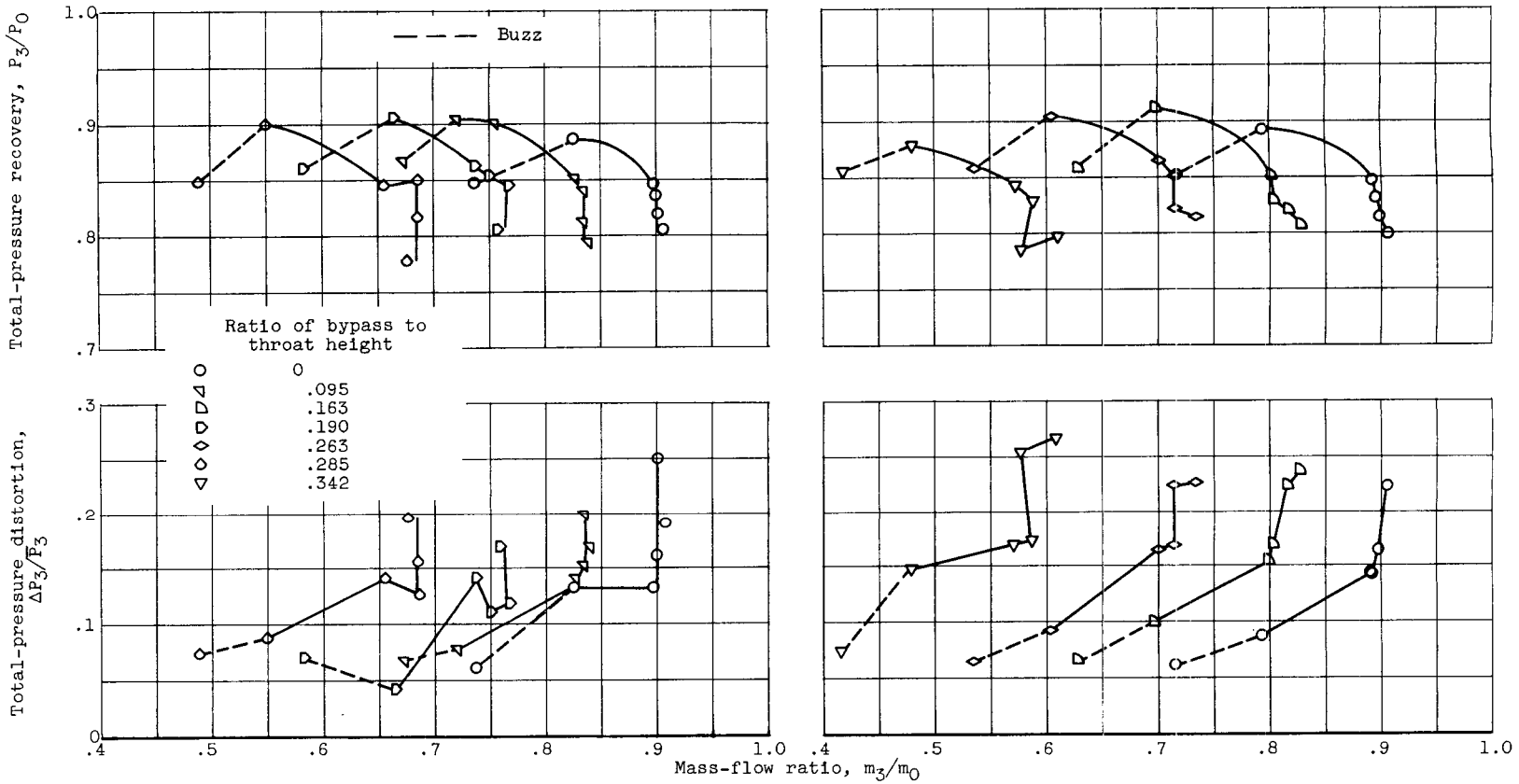

(c) Top bypass without flow divider. Ratio of scoop to throat height, 0.062.

(d) Bottom bypass with short diffuser plate. Ratio of scoop to throat height, 0.062.

Figure 7. - Concluded. Performance of two-shock ramp ($5\frac{3^\circ}{4}$ and $20\frac{3^\circ}{4}$) with different bypasses at Mach 1.89.

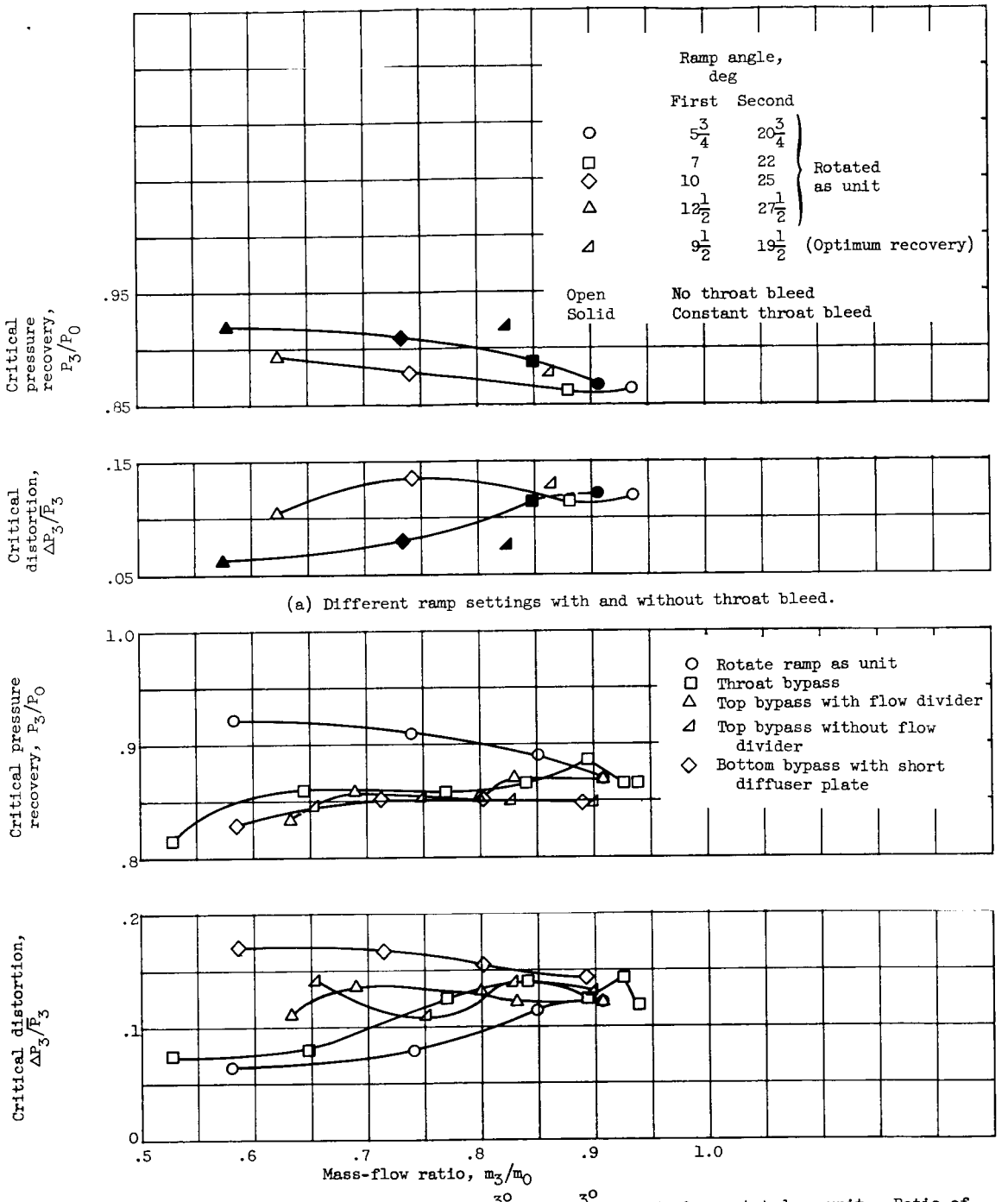

(a) Different ramp settings with and without throat bleed.

(b) All match methods. Ramps set at $5\frac{3}{4}^{\circ}$ and $20\frac{3}{4}^{\circ}$ except when rotated as unit. Ratio of scoop to throat height, 0.062 except with throat bypass.

Figure 8. - Summary of critical performances of two-shock ramp at Mach 1.89.

[redacted]

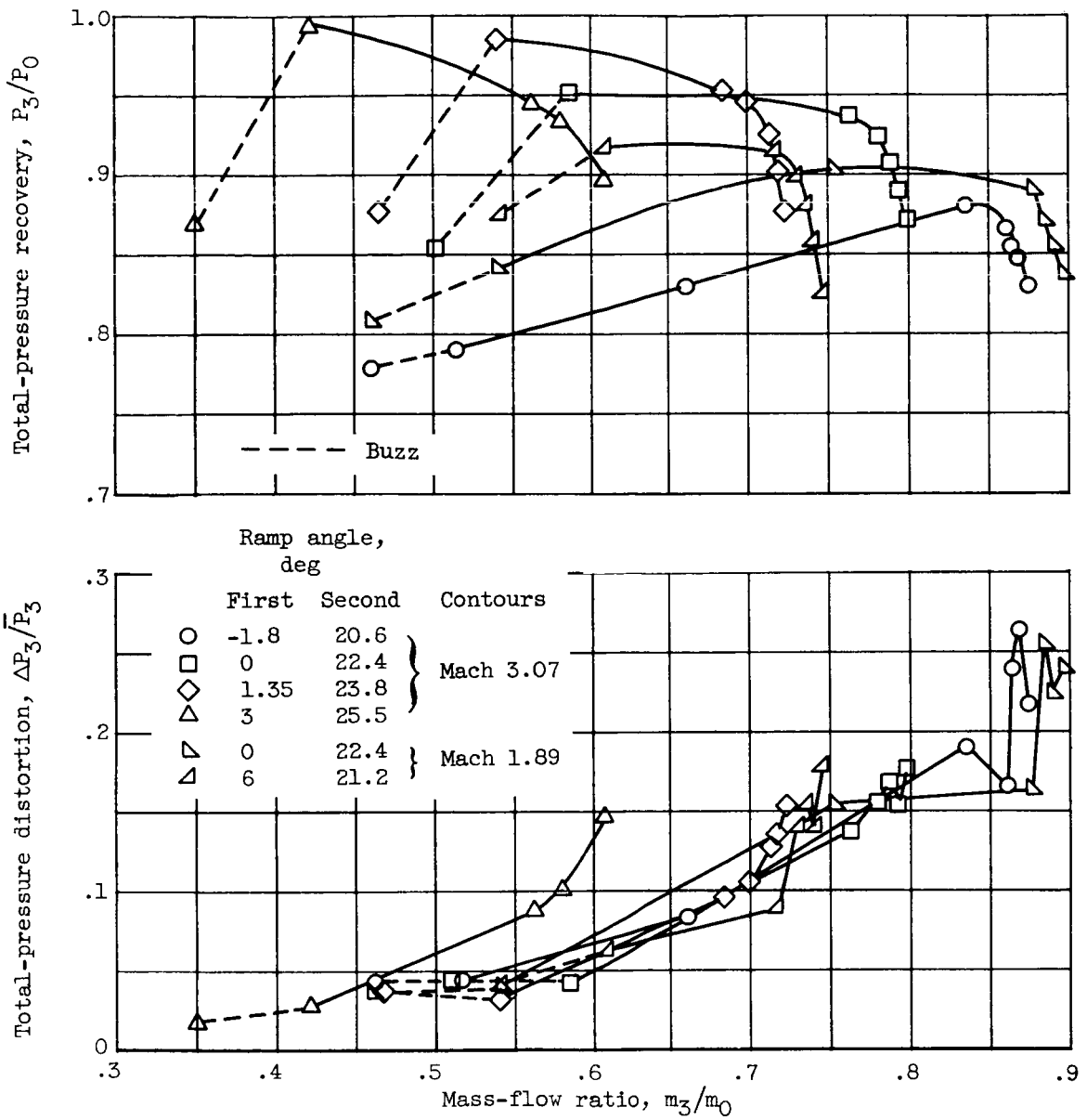

Figure 9. - Performance of isentropic ramp with different ramp settings and contours with constant scoop height at Mach 1.89.

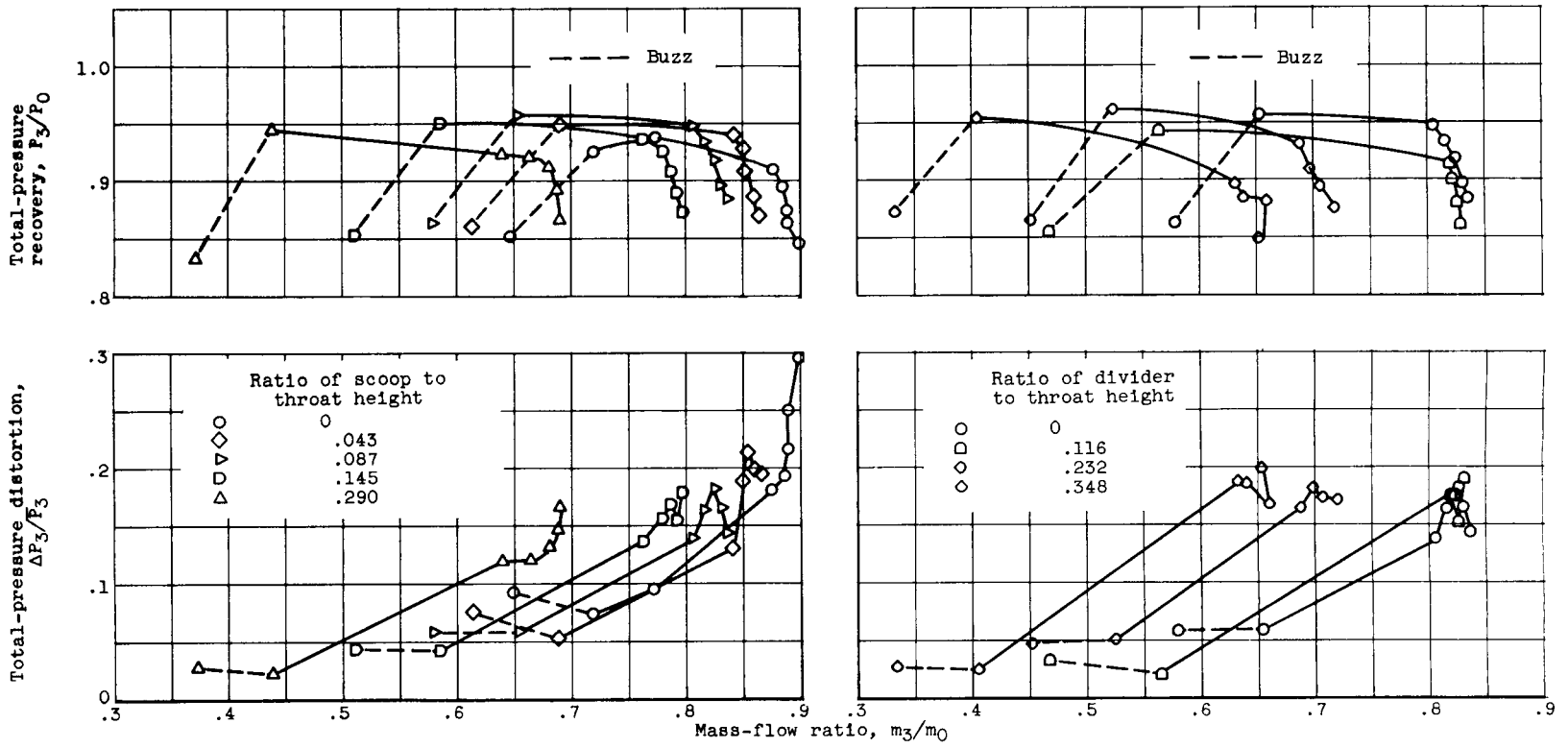

(a) Throat bypass.

(b) Top bypass with flow divider. Ratio of scoop to throat height, 0.087.

Figure 10. - Performance of isentropic ramp with Mach 3.07 contour (0° and 22.4°) with different bypasses at Mach 1.89.

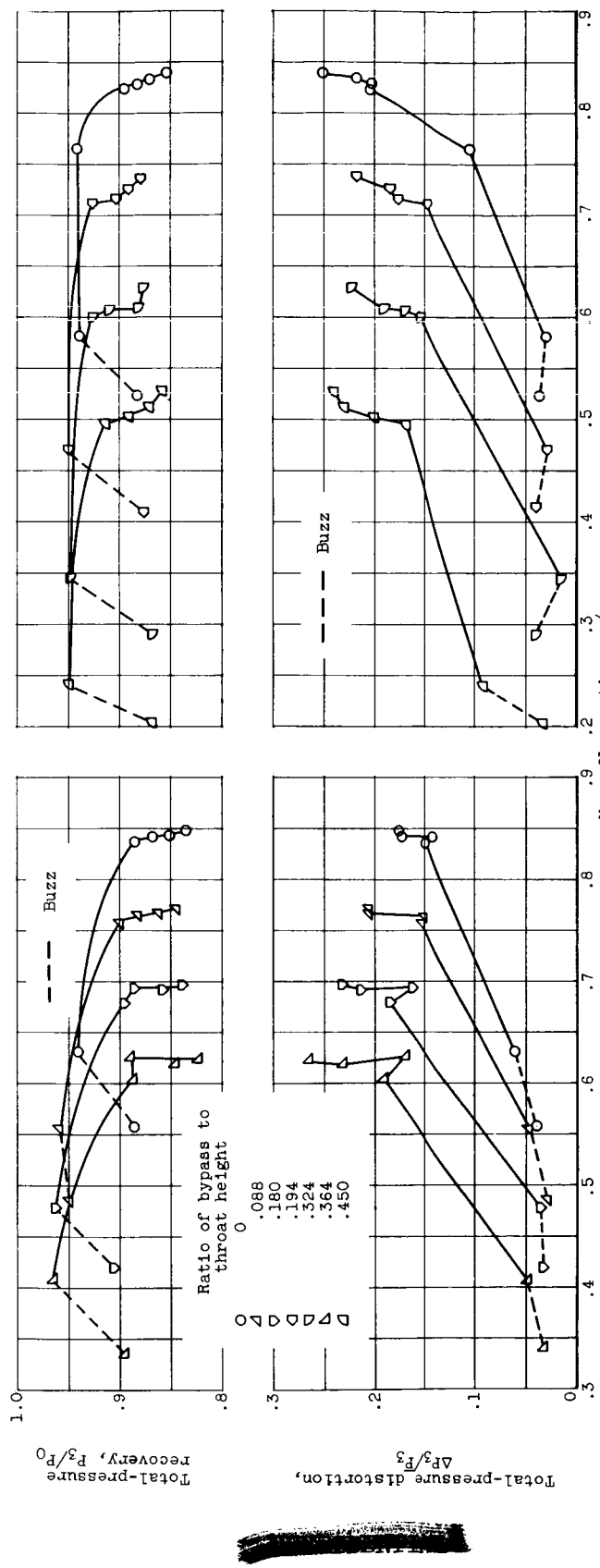

(c) Top bypass without flow divider. Ratio of scoop to throat height, 0.087.

(d) Bottom bypass with short diffuser plate. Ratio of scoop to throat height, 0.087.

Figure 10. - Concluded. Performance of isentropic ramp with Mach 3.07 contour (0° and 22.4°) with different bypasses at Mach 1.89.

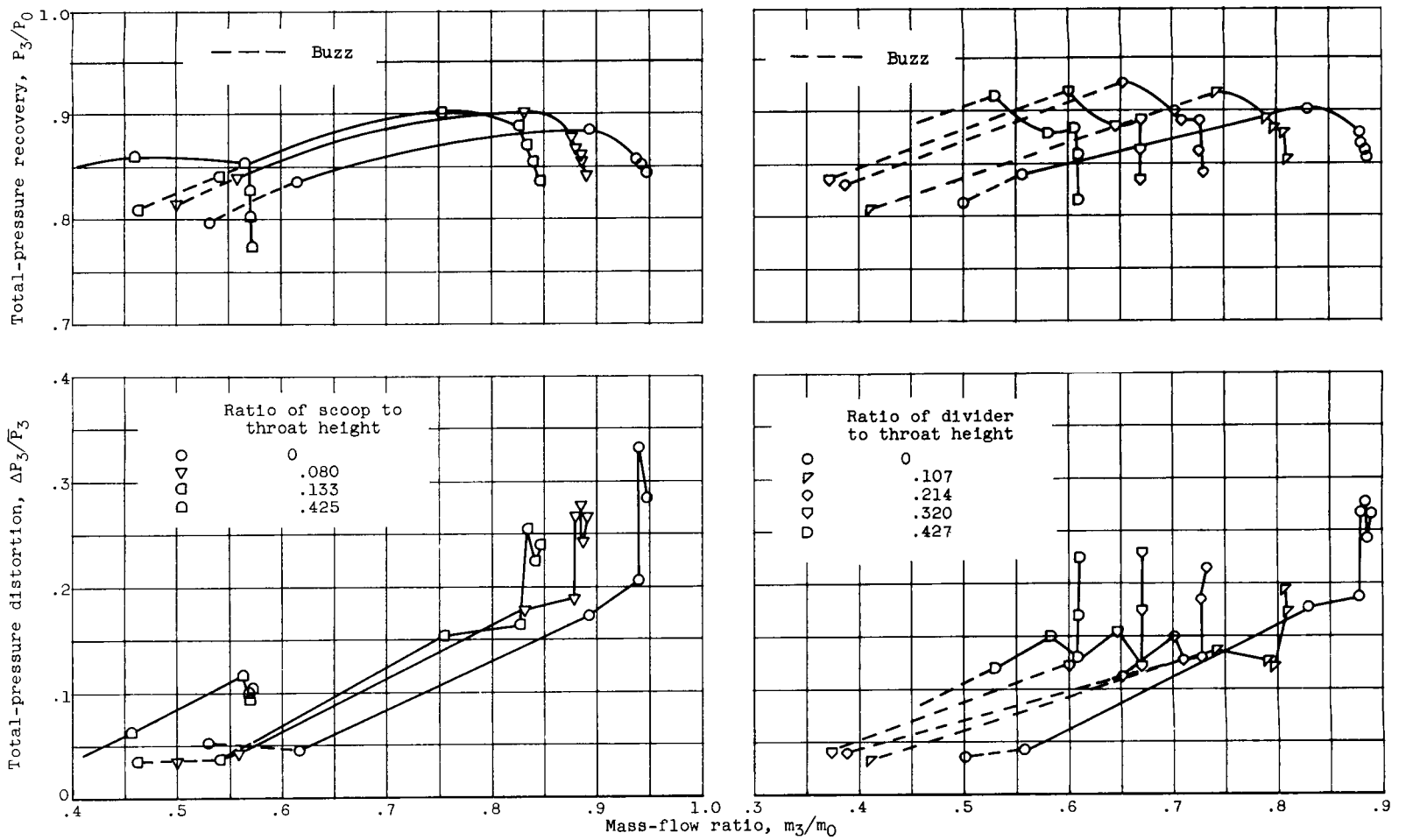

(a) Throat bleed.

(b) Top bypass with flow divider. Ratio of scoop to throat height, 0.08.

Figure 11. - Performance of isentropic ramp with Mach 1.89 contour (0° and 22.4°) with different bypasses at Mach 1.89.

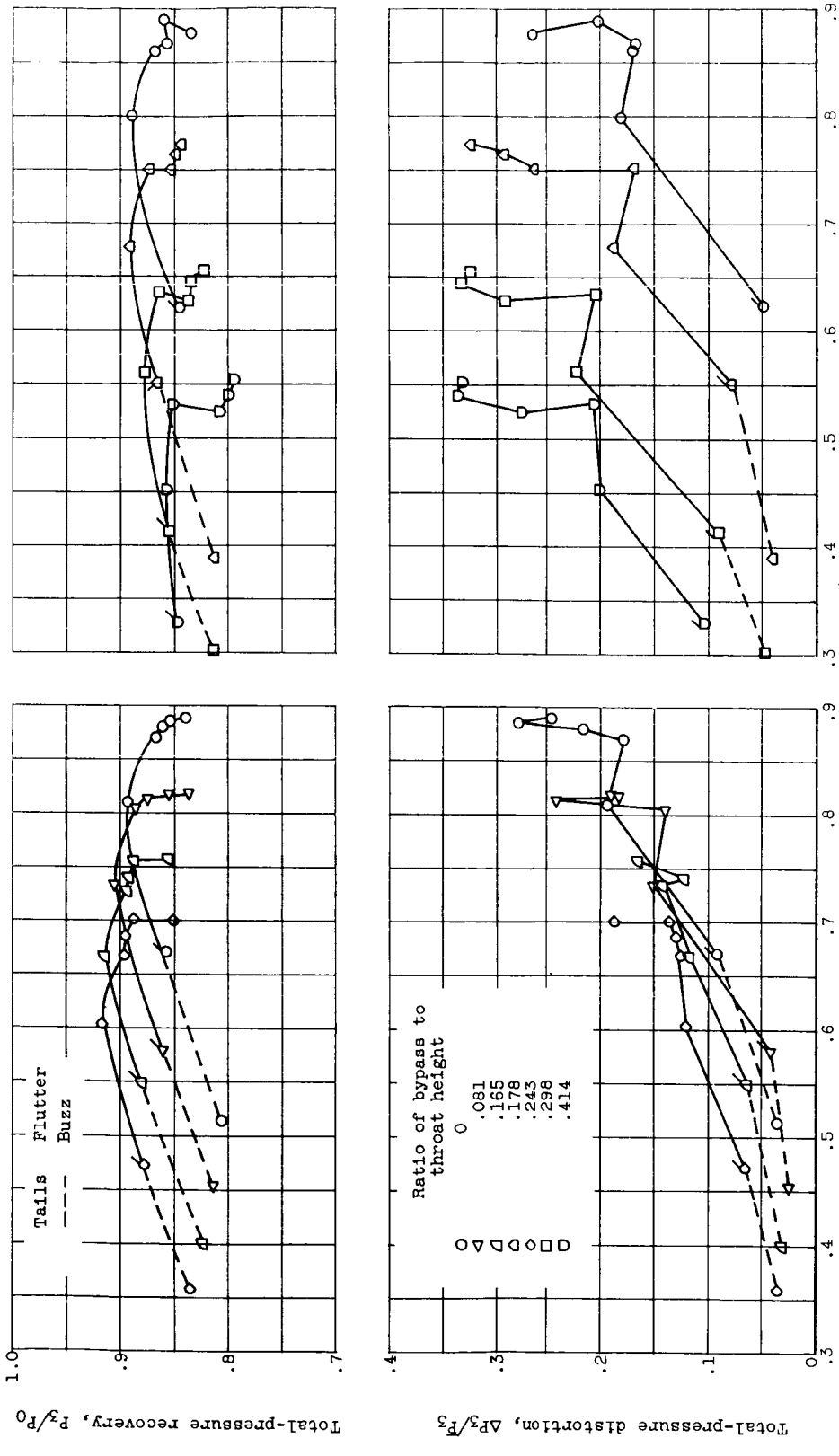

(c) Top bypass without flow divider. Ratio of scoop to throat height, 0.08.

(d) Bottom bypass with short diffuser plate. Ratio of scoop to throat height, 0.08.

Figure 11. - Concluded. Performance of isentropic ramp with Mach 1.89 contour (0° and 22.4°) with different bypasses at Mach 1.8[illegible].

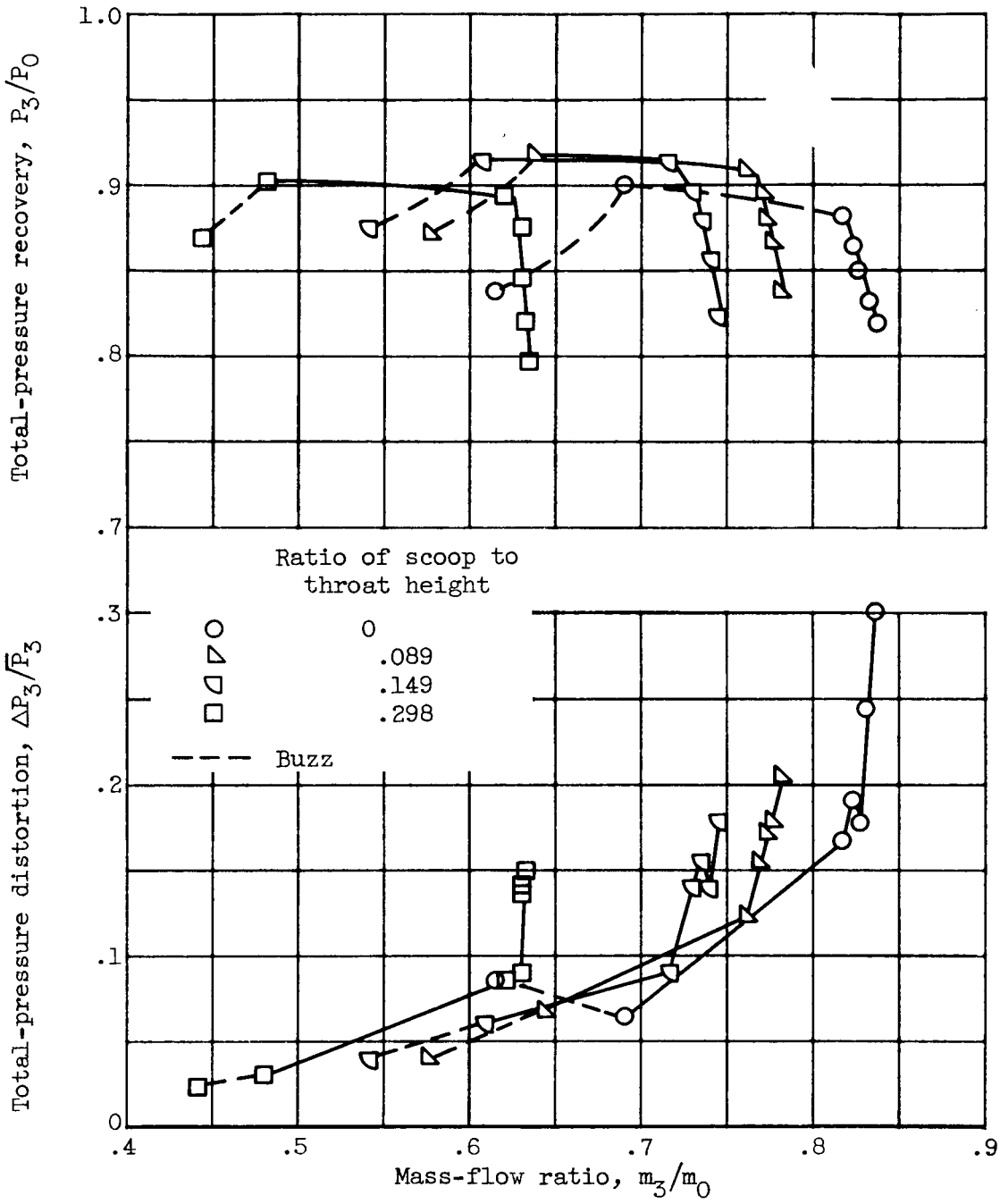

Figure 12. - Performance of isentropic ramp with Mach 1.89 contour (6° and 21.2°) with different ratios of scoop to throat height at Mach 1.89.

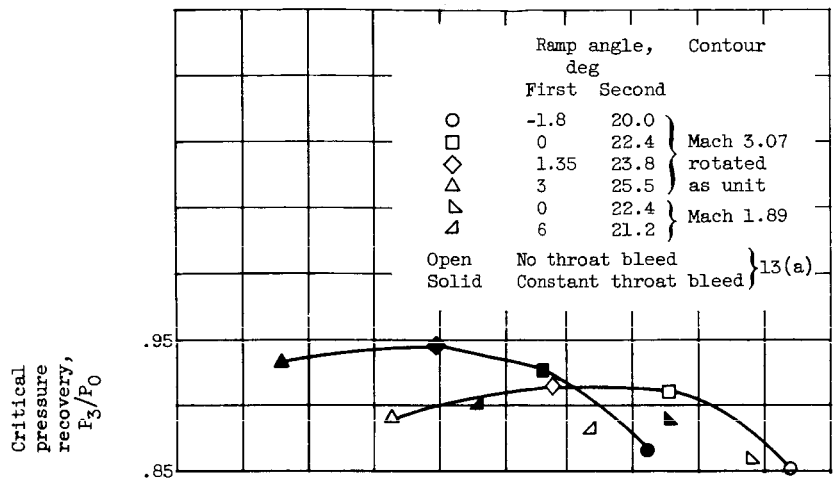

(a) Different ramp settings with and without throat bleed.

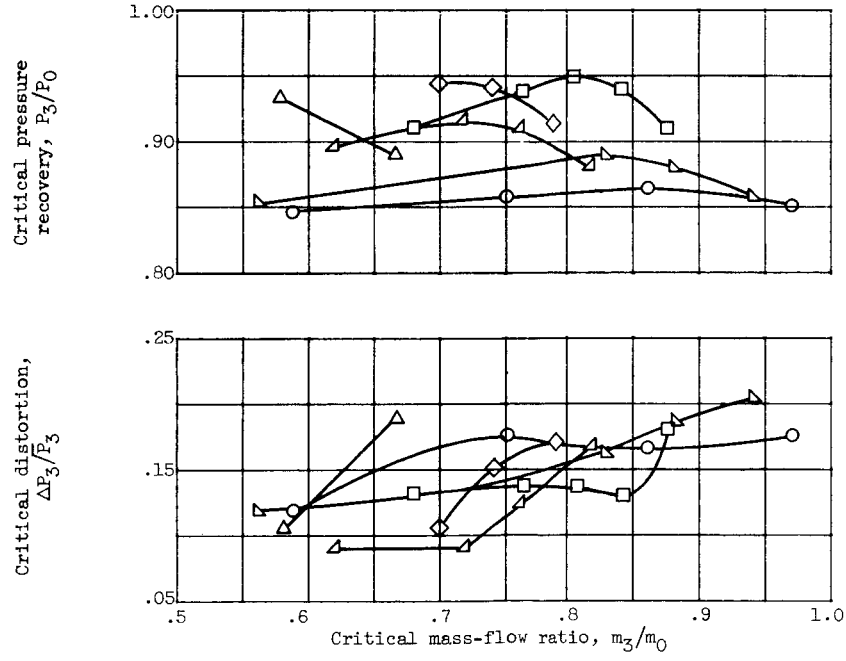

(b) All contour settings with varying throat bleed.

Figure 13. - Summary of critical performance of isentropic ramp at Mach 1.89.

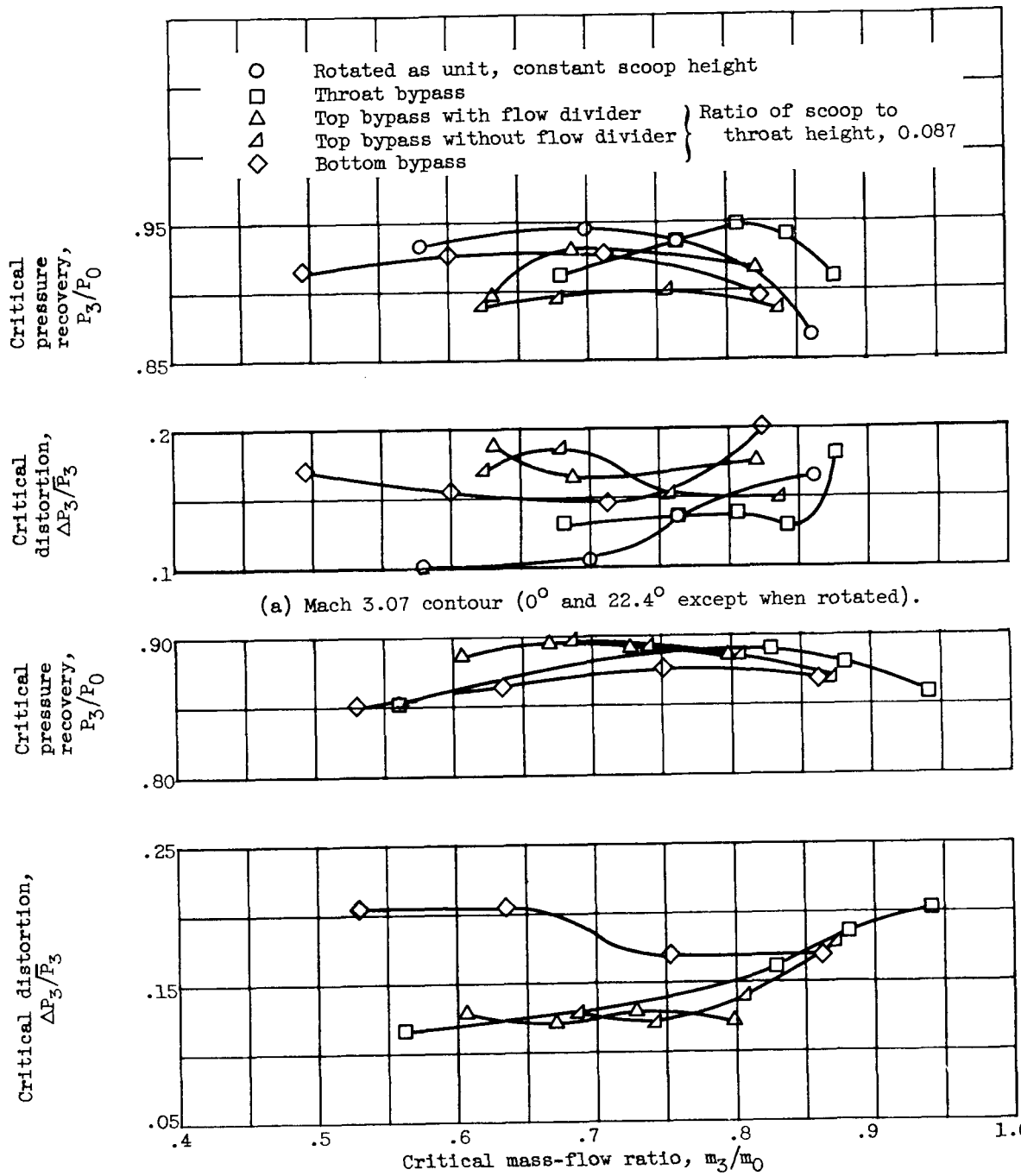

(a) Mach 3.07 contour (0° and 22.4° except when rotated).

(b) Mach 1.89 contour (0° and 22.4°). Ratio of scoop to throat height, 0.08, except with throat bypass.

Figure 14. - Summary of critical performance of isentropic ramp with all bypass arrangements at Mach 1.89.

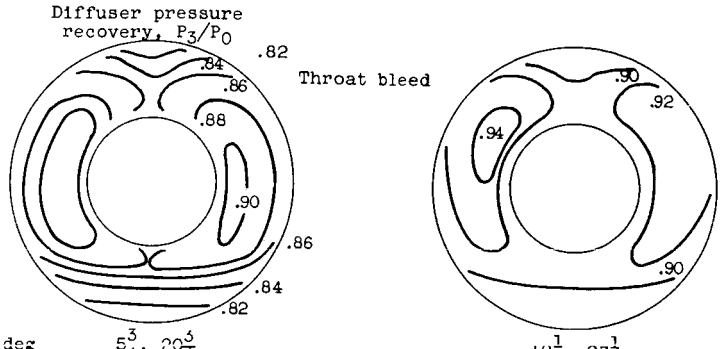

Ramp angles, deg	$5\frac{3}{4}$, $20\frac{3}{4}$	$12\frac{1}{2}$, $27\frac{1}{2}$
$\bar{P}_3/P_0$	0.87	0.92
m_3/m_0	0.91	0.58
$\Delta P_3/\bar{P}_3$	0.125	0.065

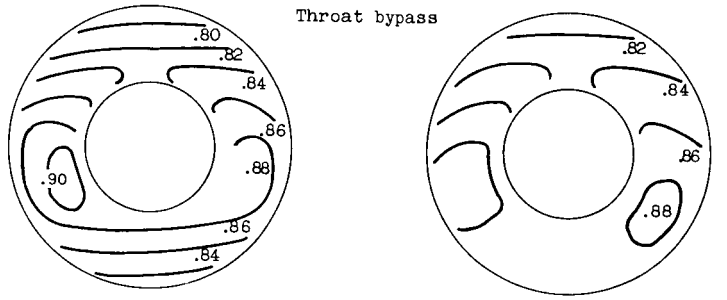

Scoop height / Throat height	0.250	0.375
Ramp angles, deg	$5\frac{3}{4}$, $20\frac{3}{4}$	$5\frac{3}{4}$, $20\frac{3}{4}$
$\bar{P}_3/P_0$	0.86	0.86
m_3/m_0	0.77	0.65
$\Delta P_3/\bar{P}_3$	0.125	0.08

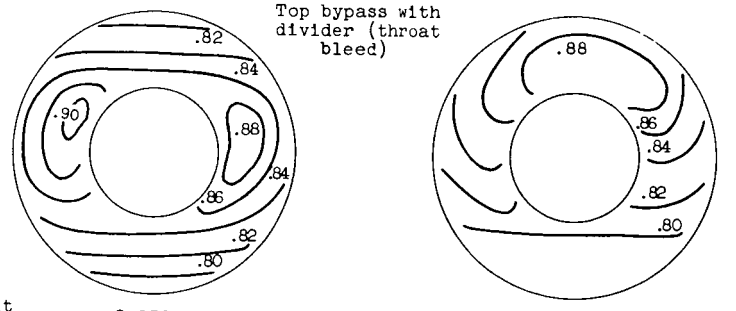

Divider height / Throat height	0.250	0.500
Ramp angles, deg	$5\frac{3}{4}$, $20\frac{3}{4}$	$5\frac{3}{4}$, $20\frac{3}{4}$
$\bar{P}_3/P_3$	0.85	0.84
m_3/m_0	0.80	0.63
$\Delta P_3/\bar{P}_3$	0.13	0.11

Figure 15. - Critical pressure-recovery contours at compressor face with two-shock ramp and different matching methods.

Top bypass without divider (throat bleed)

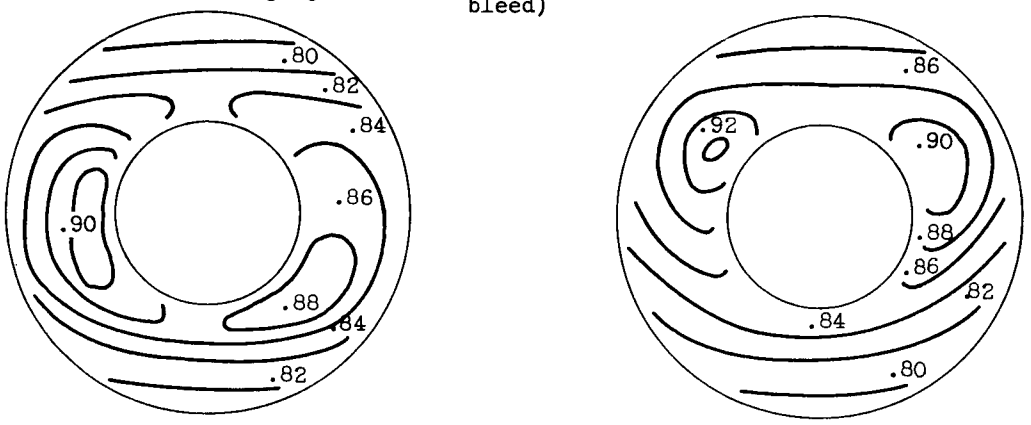

Bypass height / Throat height	0.095	0.190
Ramp angles, deg	$5\frac{3}{4}$, $20\frac{3}{4}$	$5\frac{3}{4}$, $20\frac{3}{4}$
$\overline{P}_3/P_0$	0.85	0.86
m_3/m_0	0.83	0.74
$\Delta P_3/\overline{P}_3$	0.14	0.14

Bottom bypass with short diffuser plate (throat bleed)

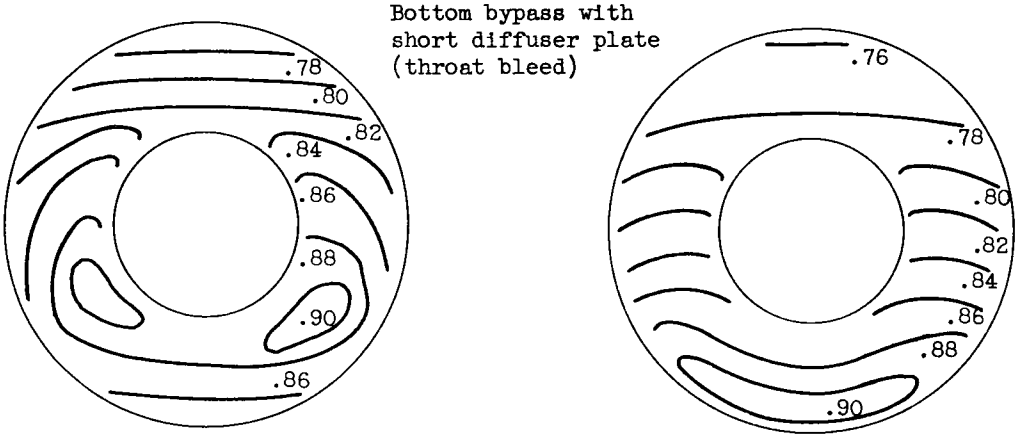

Bypass height / Throat height	0.163	0.342
Ramp angles, deg	$5\frac{3}{4}$, $20\frac{3}{4}$	$5\frac{3}{4}$, $20\frac{3}{4}$
$\overline{P}_3/P_0$	0.85	0.83
m_3/m_0	0.80	0.59
$\Delta P_3/\overline{P}_3$	0.15	0.17

Figure 15. - Concluded. Critical pressure-recovery contours at compressor face with two-shock ramp and different matching methods.

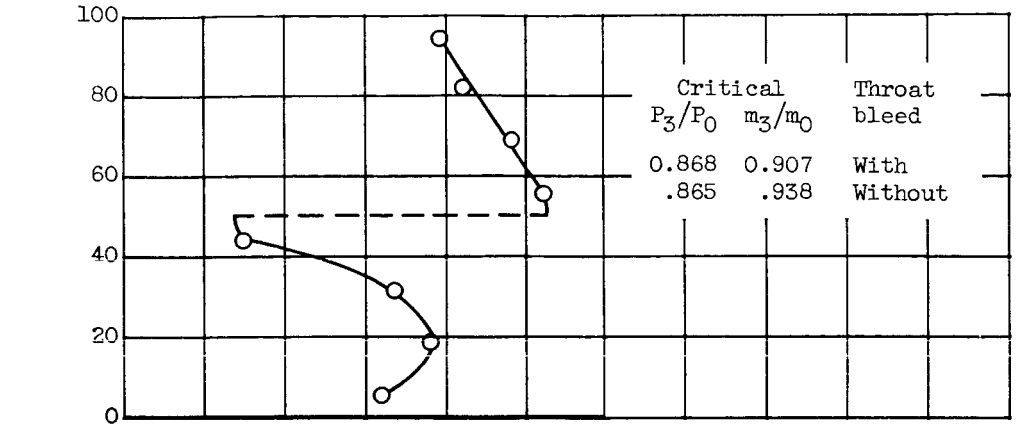

(a) Two-shock ramp ($5\frac{3^\circ}{4}$ and $20\frac{30^\circ}{4}$).

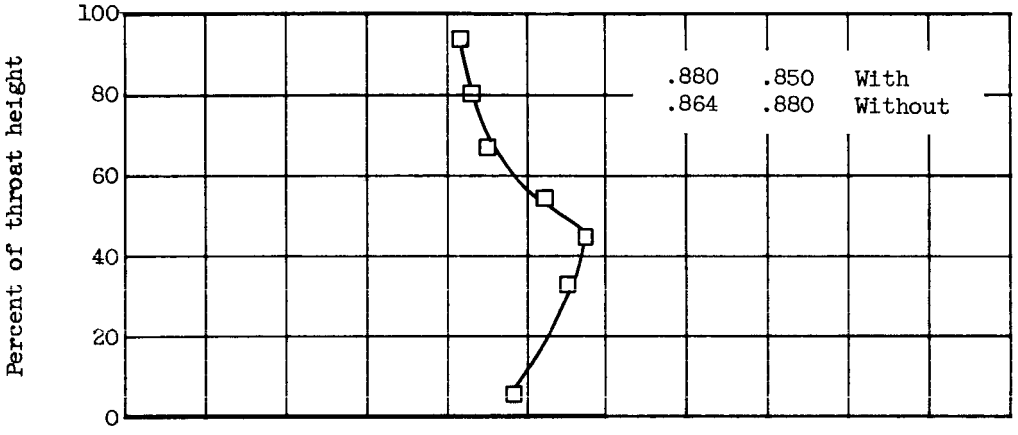

(b) Two-shock ramp (7° and 22°).

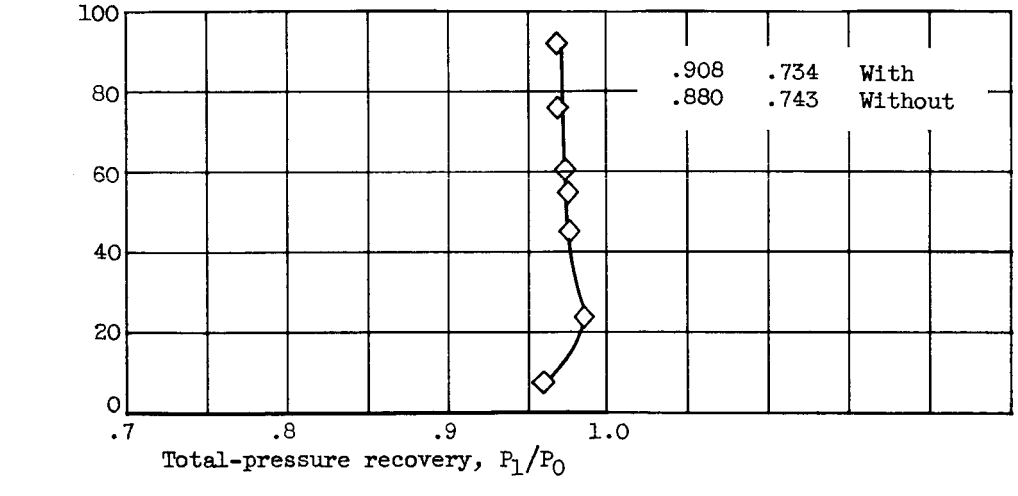

(c) Two-shock ramp (10° and 25°).

Figure 16. - Total-pressure profiles at throat during critical operation at Mach 1.89.

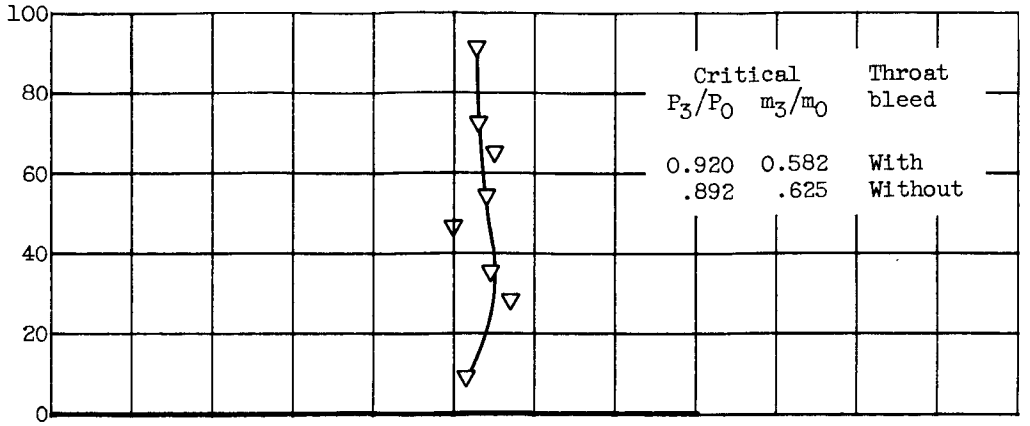

(d) Two-shock ramp ($12\frac{1}{2}^\circ$ and $27\frac{1}{2}^\circ$).

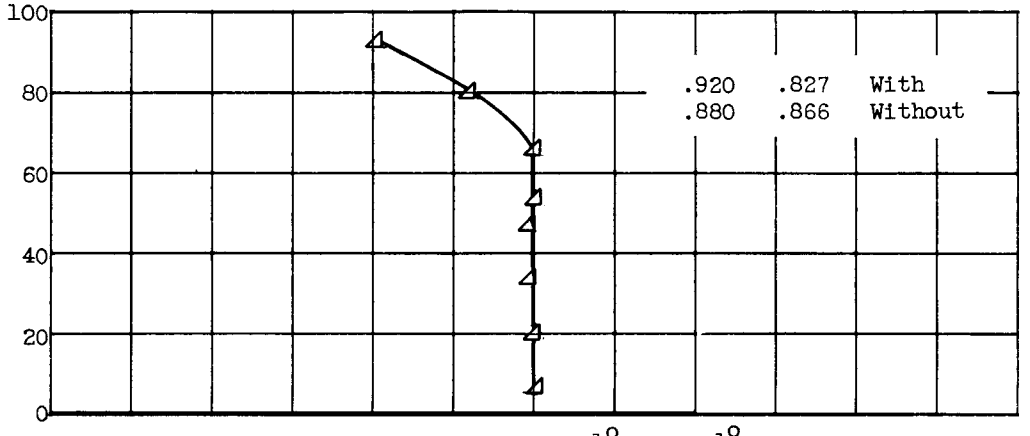

(e) Two-shock ramp ($9\frac{1}{2}^\circ$ and $19\frac{1}{2}^\circ$).

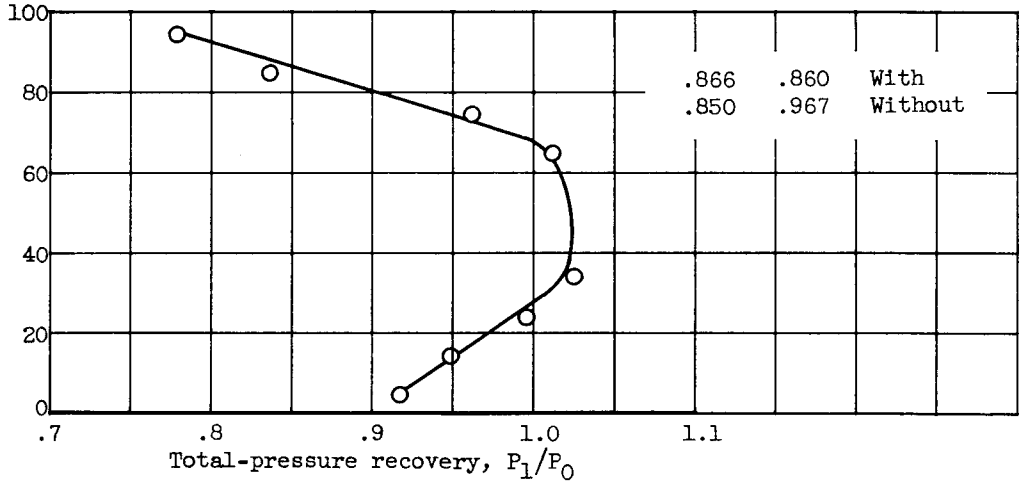

(f) Isentropic ramp with Mach 3.07 contour (-1.8° and 20.6°).

Figure 16. - Continued. Total-pressure profiles at throat during critical operation at Mach 1.89.

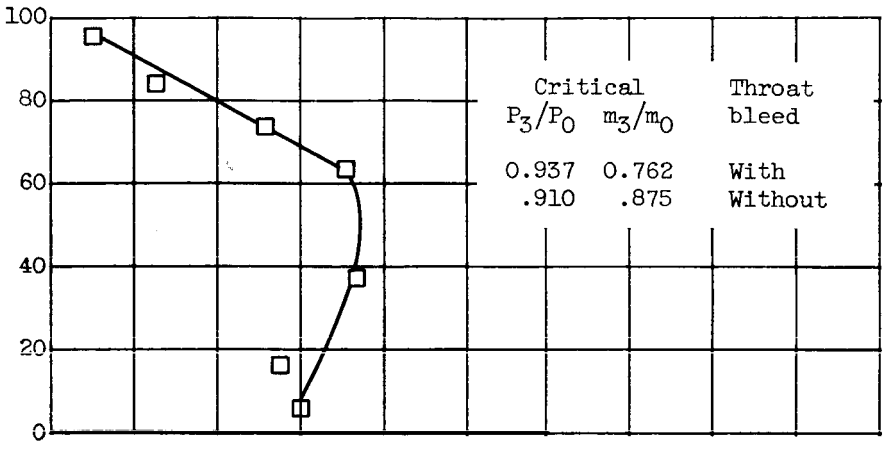

(g) Isentropic ramp with Mach 3.07 contour (0° and 22.4°).

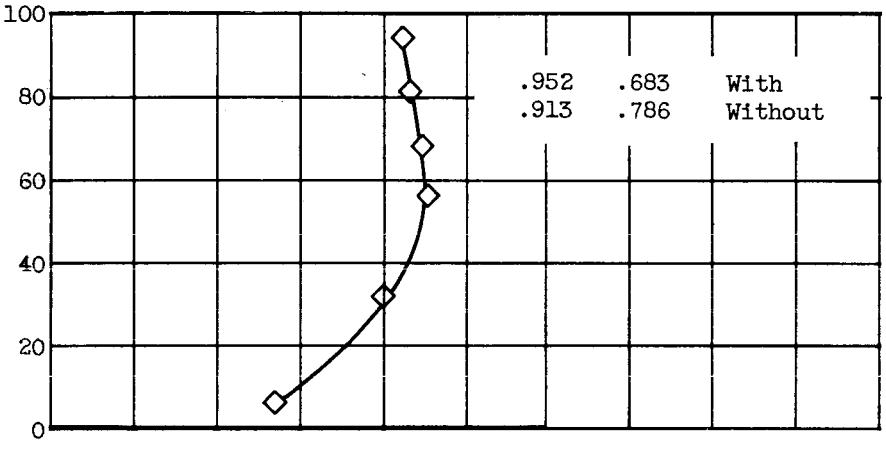

Percent of throat height

(h) Isentropic ramp with Mach 3.07 contour (1.35° and 23.8°).

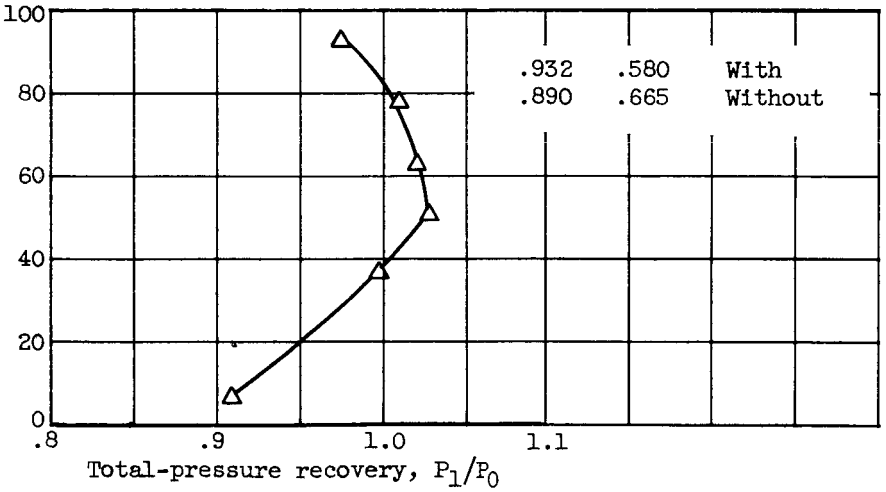

(i) Isentropic ramp with Mach 3.07 contour (3° and 25.5°).

Figure 16. - Continued. Total-pressure profiles at throat during critical operation at Mach 1.89.

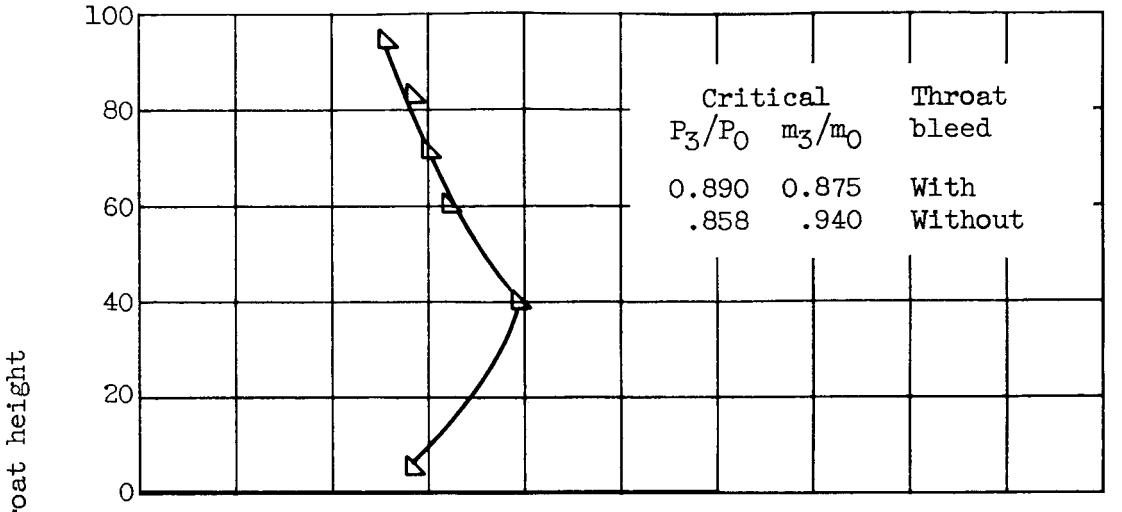

(j) Isentropic ramp with Mach 1.89 contour (0° and 22.4°).

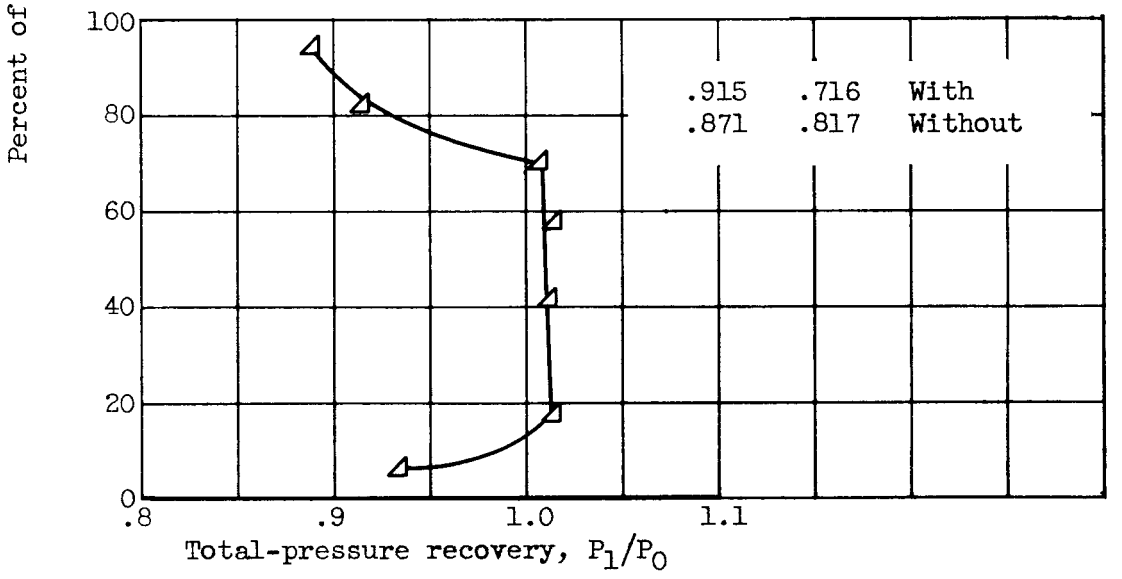

(k) Isentropic ramp with Mach 1.89 contour (6° and 21.2°).

Figure 16. - Concluded. Total-pressure profiles at throat during critical operation at Mach 1.89.

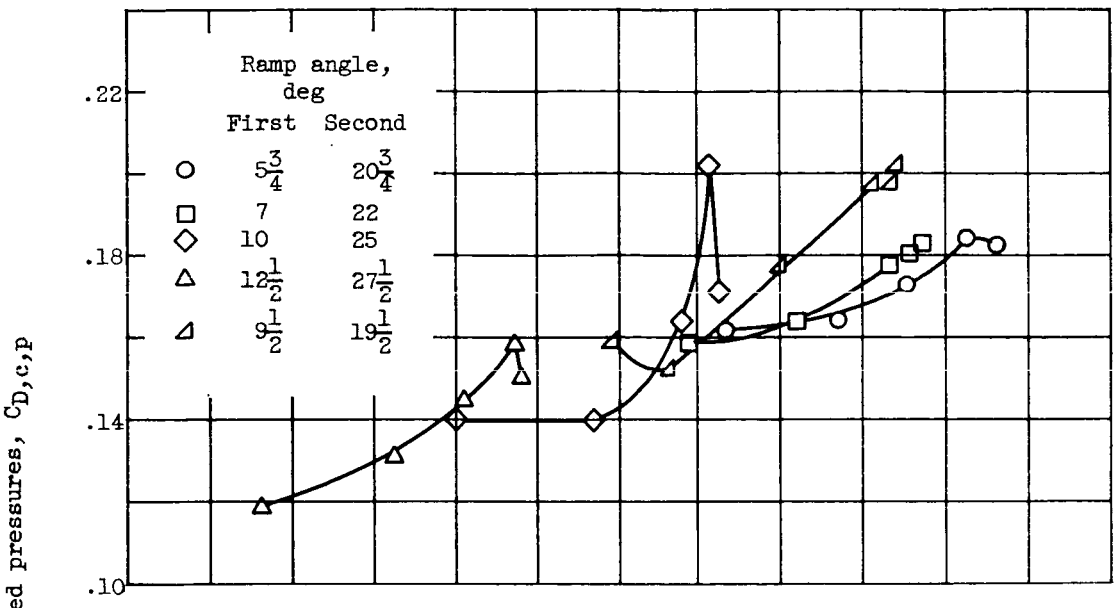

(a) Two-shock ramp with different ramp angles.

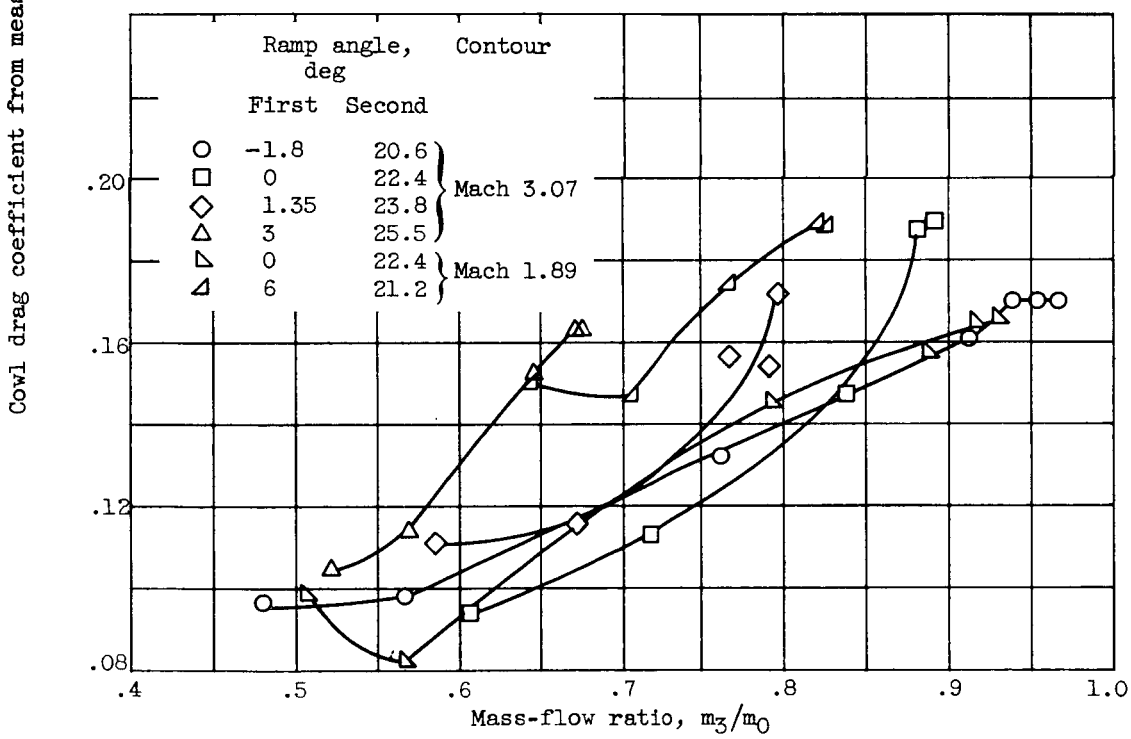

(b) Isentropic ramp with different ramp contours and settings.

Figure 17. - Measured cowl pressure-drag coefficients based on compressor frontal area at Mach 1.89.

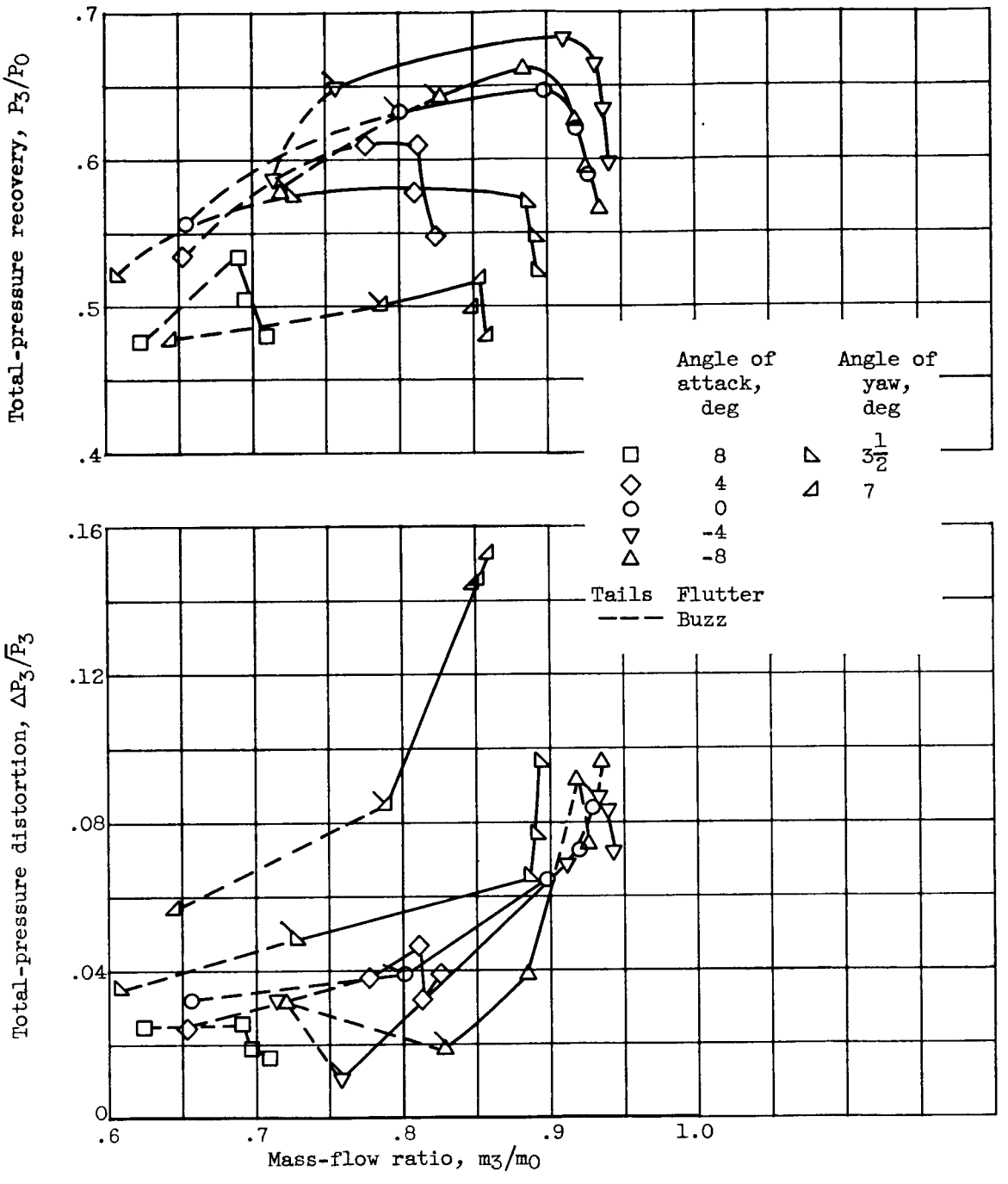

Figure 18. - Mach 3.07 performance of two-shock ramp (15° and 30°) with ratio of scoop to throat height of 0.116 at angles of attack and yaw.

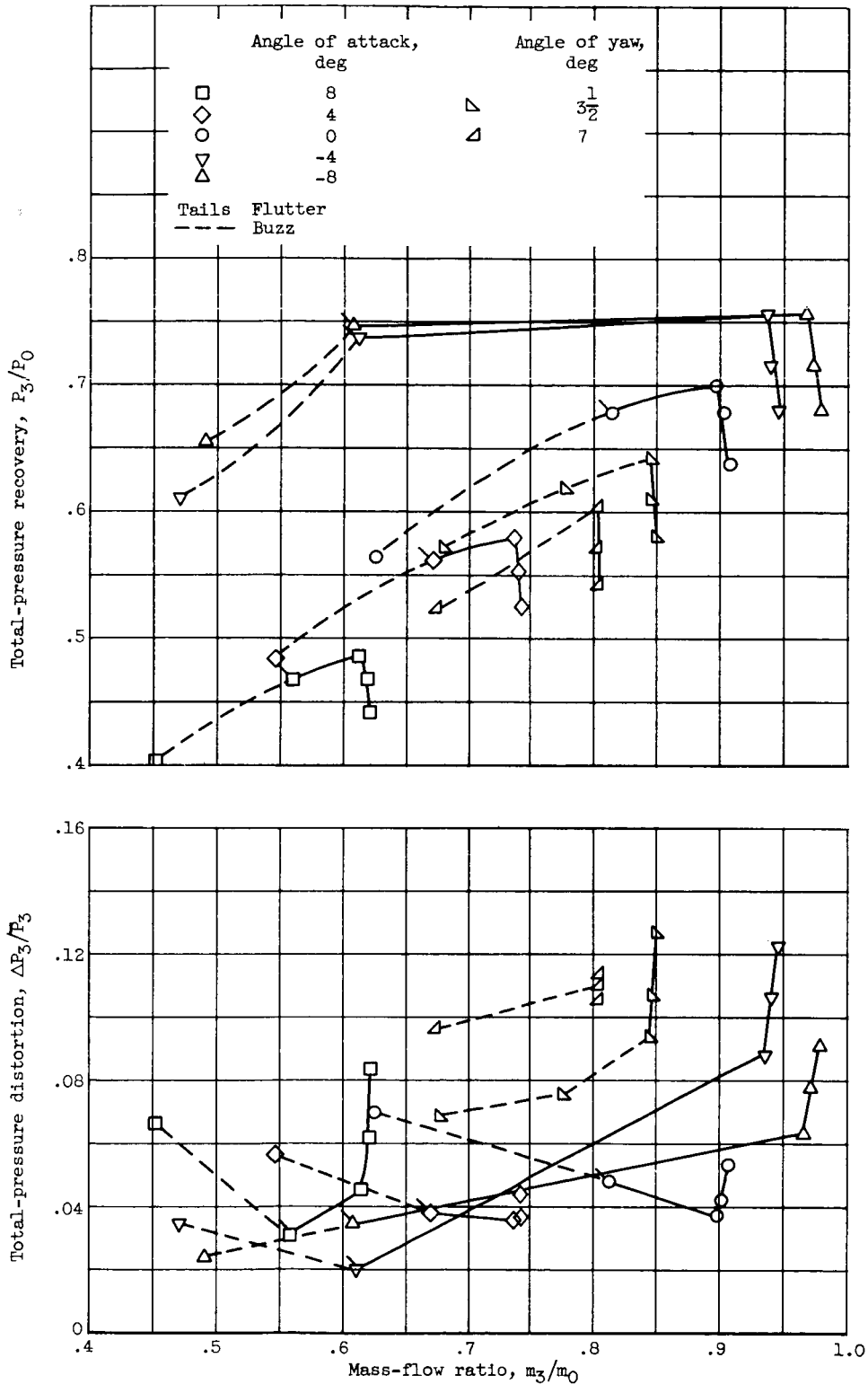

Figure 19. - Mach 3.07 performance of isentropic ramp (6° and 28.4°) with ratio of scoop to throat height of 0.240 at angles of attack and yaw.

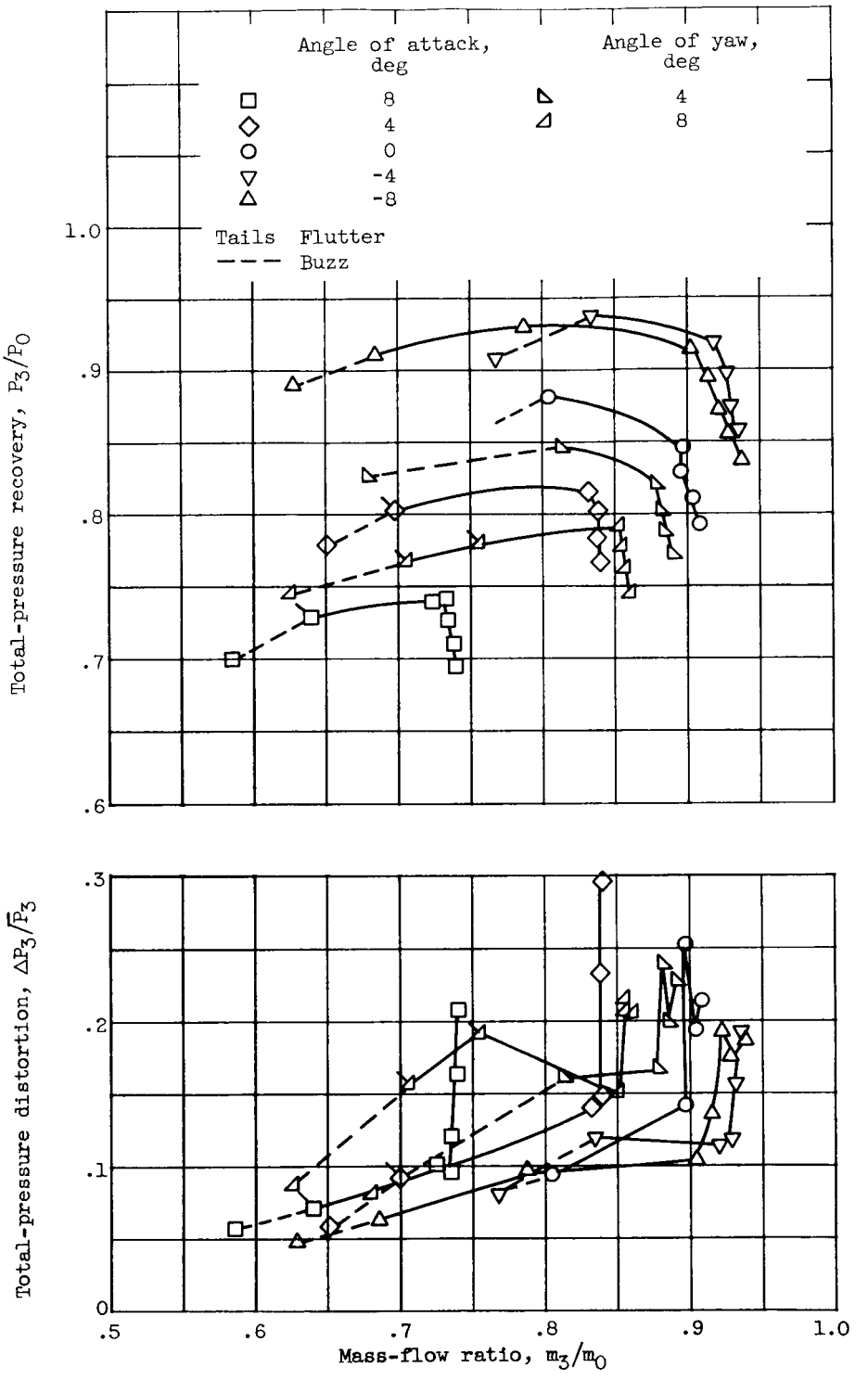

(a) No bypass. Ratio of scoop to throat height, 0.062.

Figure 20. - Mach 1.89 performance of two-shock ramp ($5\frac{3^\circ}{4}$ and $20\frac{3^\circ}{4}$) at angles of attack and yaw.

[redacted]

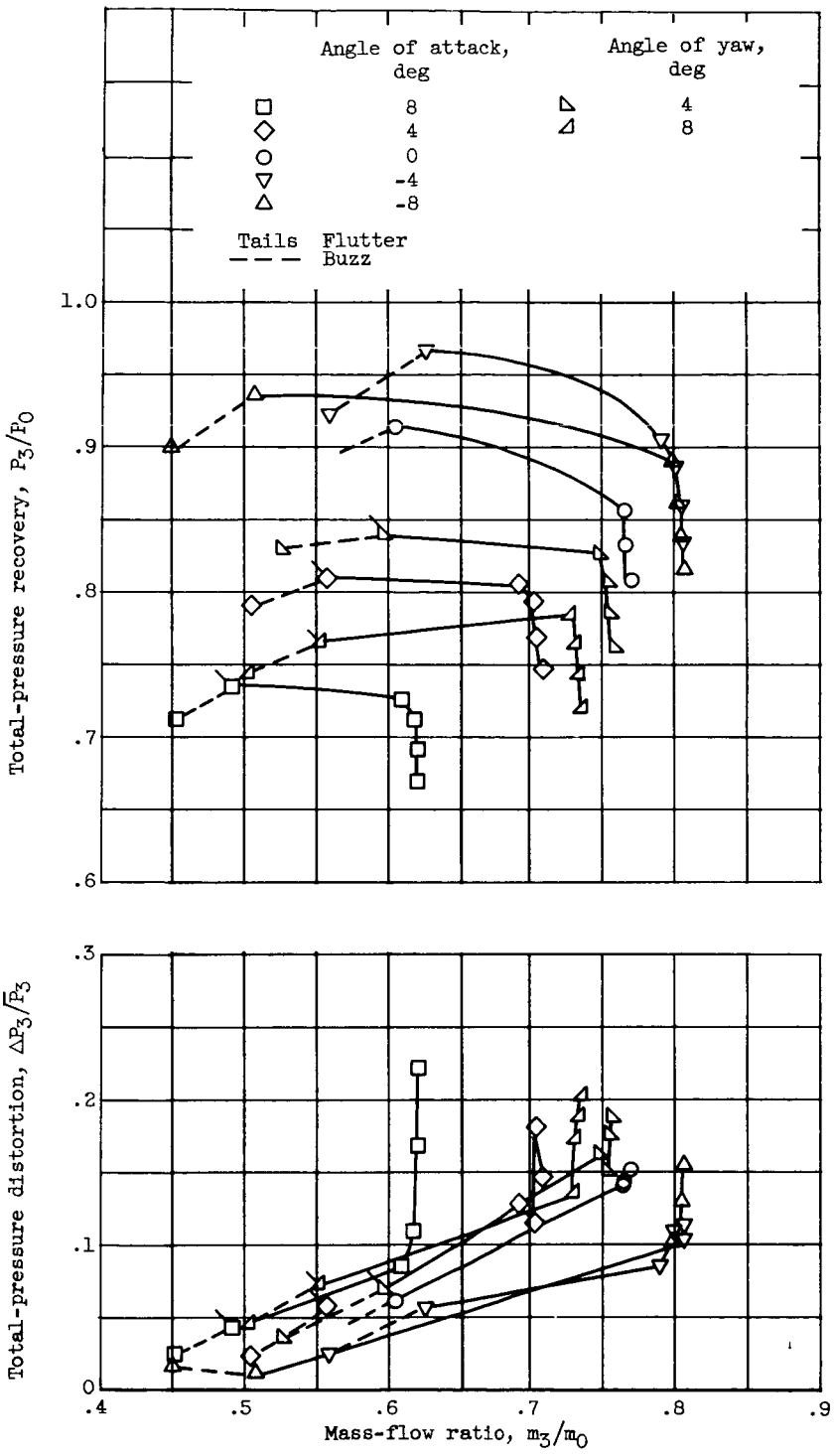

(b) Throat bypass. Ratio of scoop to throat height, 0.250.

Figure 20. - Continued. Mach 1.89 performance of two-shock ramp ($5\frac{3^\circ}{4}$ and $20\frac{3^\circ}{4}$) at angles of attack and yaw.

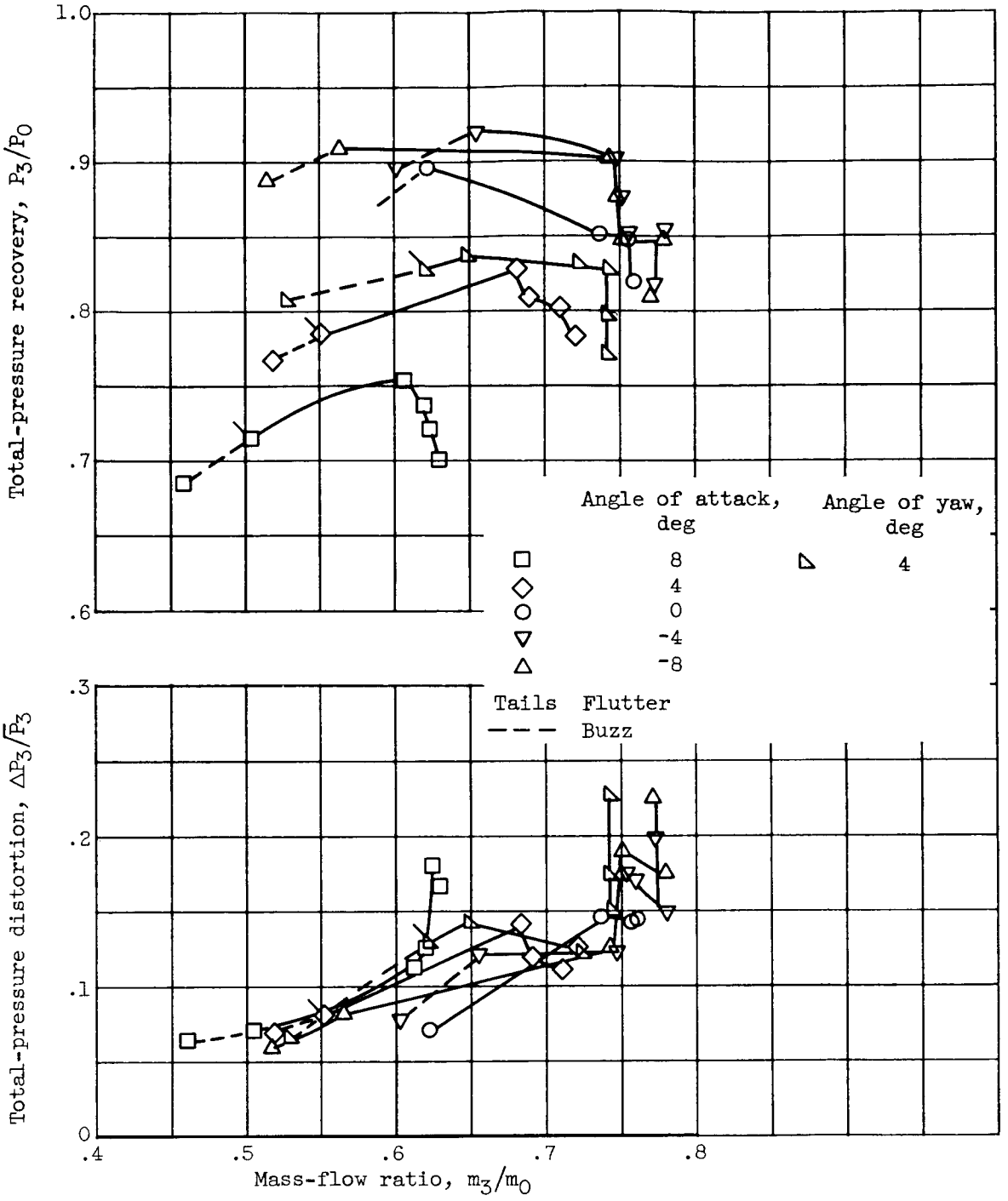

(c) Top bypass with flow divider. Ratio of divider to throat height, 0.250; ratio of scoop to throat height, 0.062.

Figure 20. - Concluded. Mach 1.89 performance of two-shock ramp ($5\frac{3^\circ}{4}$ and $20\frac{3^\circ}{4}$) at angles of attack and yaw.

[redacted]

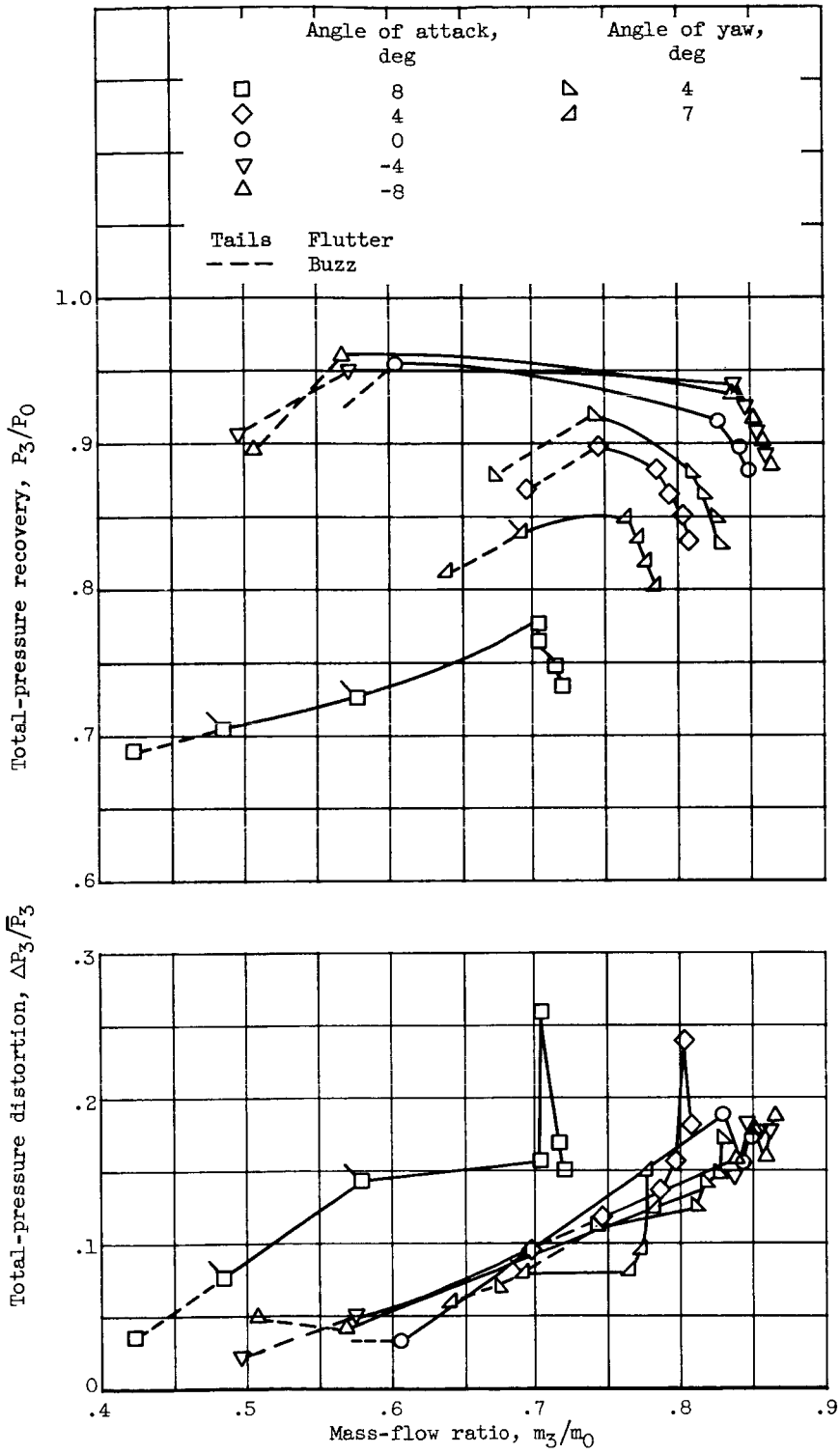

Figure 21. - Performance of isentropic ramp with Mach 3.07 contour (0° and 22.4°) at Mach 1.89 at angles of attack and yaw. Ratio of scoop to throat height, 0.087.

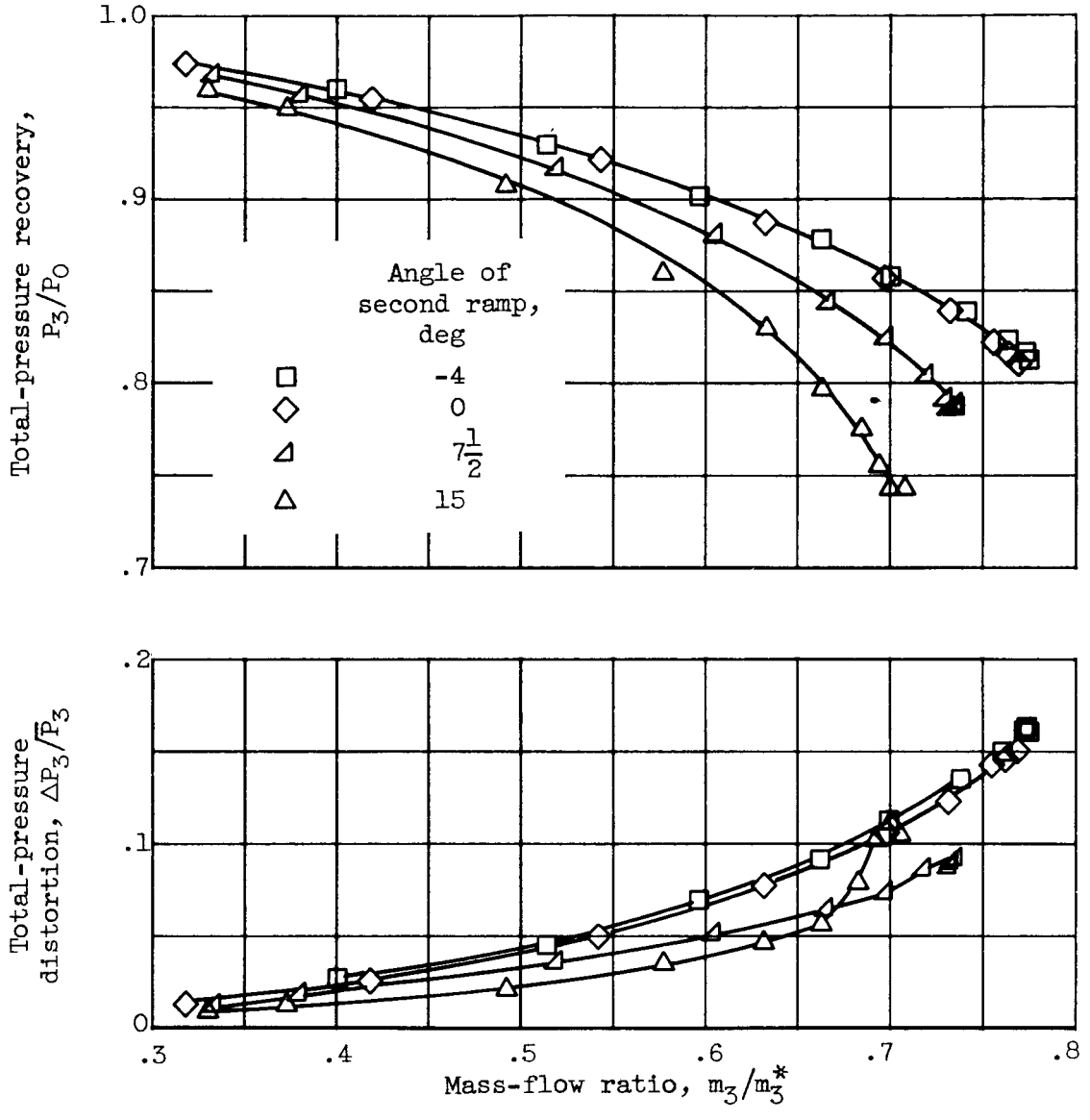

(a) No auxiliary inlet, first ramp 0°, second ramp rotated.

Figure 22. - Effect on performance of top bypass as auxiliary inlet with two-shock ramp at Mach 0.

[redacted]

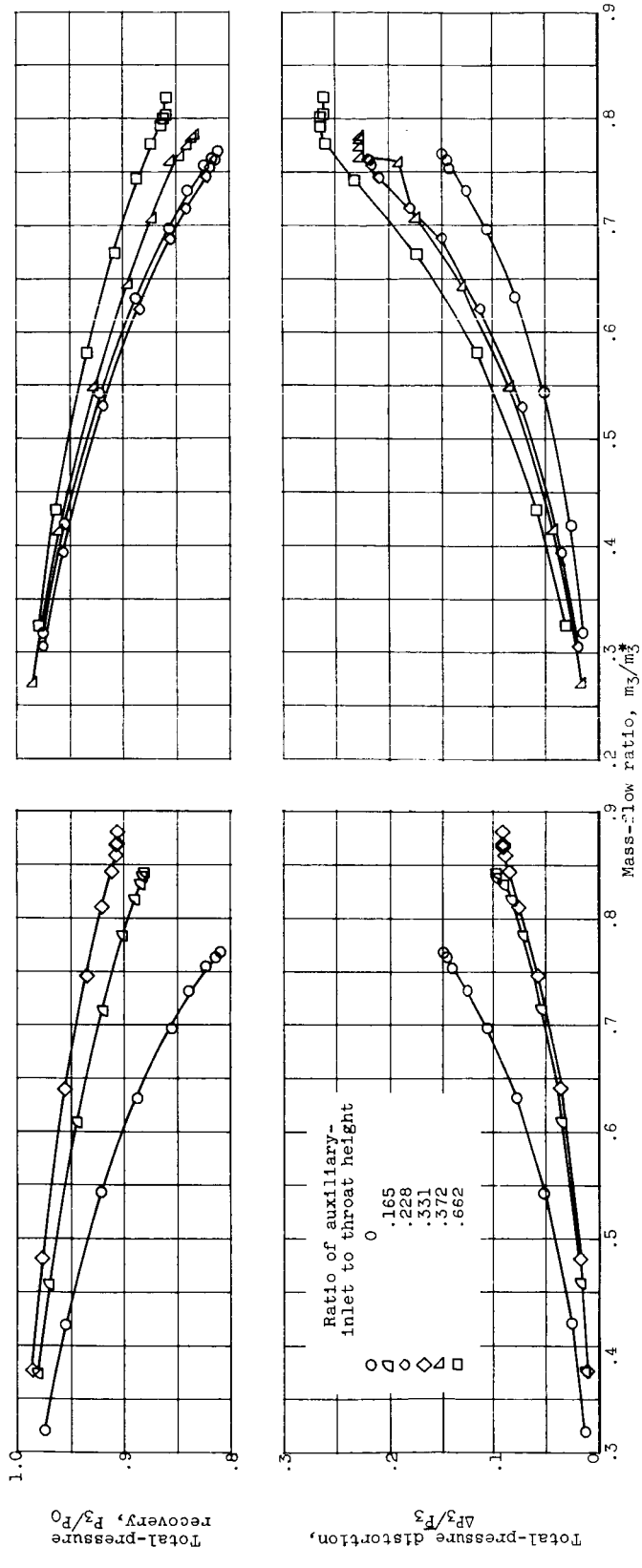

(b) Flow divider rotated into free stream, top door full open, ramp angles 0° and 0°.

(c) Top control door without flow divider, ramp angles 0° and 0°.

Figure 22. - Continued. Effect on performance of top bypass as auxiliary inlet with two-shock ramp at Mach 0.

(d) Flow divider rotated into free stream, top door full open, ramp angles 0° and $7\frac{1}{2}^\circ$.

(e) Flow divider rotated into free stream, top door full open, ramp angles 0° and 15°.

Figure 22. - Concluded. Effect on performance of top bypass as auxiliary inlet with two-shock ramp at Mach 0.

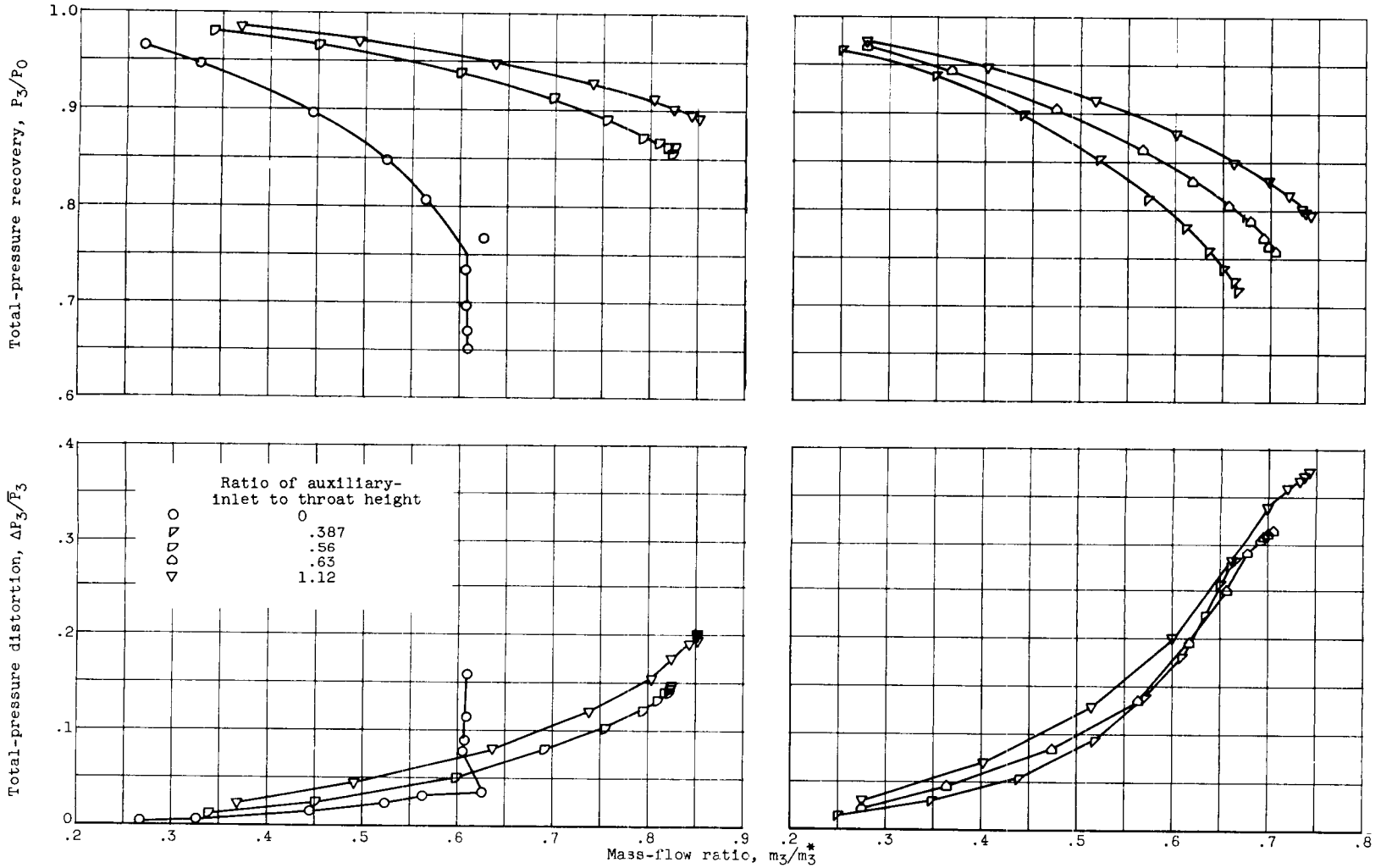

(a) Flow divider rotated into free stream, top door full open.

(b) Without flow divider; using top control door.

Figure 23. - Mach 0 performance of isentropic ramp with Mach 3.07 contour (0° and 22.4°) with top bypass as auxiliary inlet.

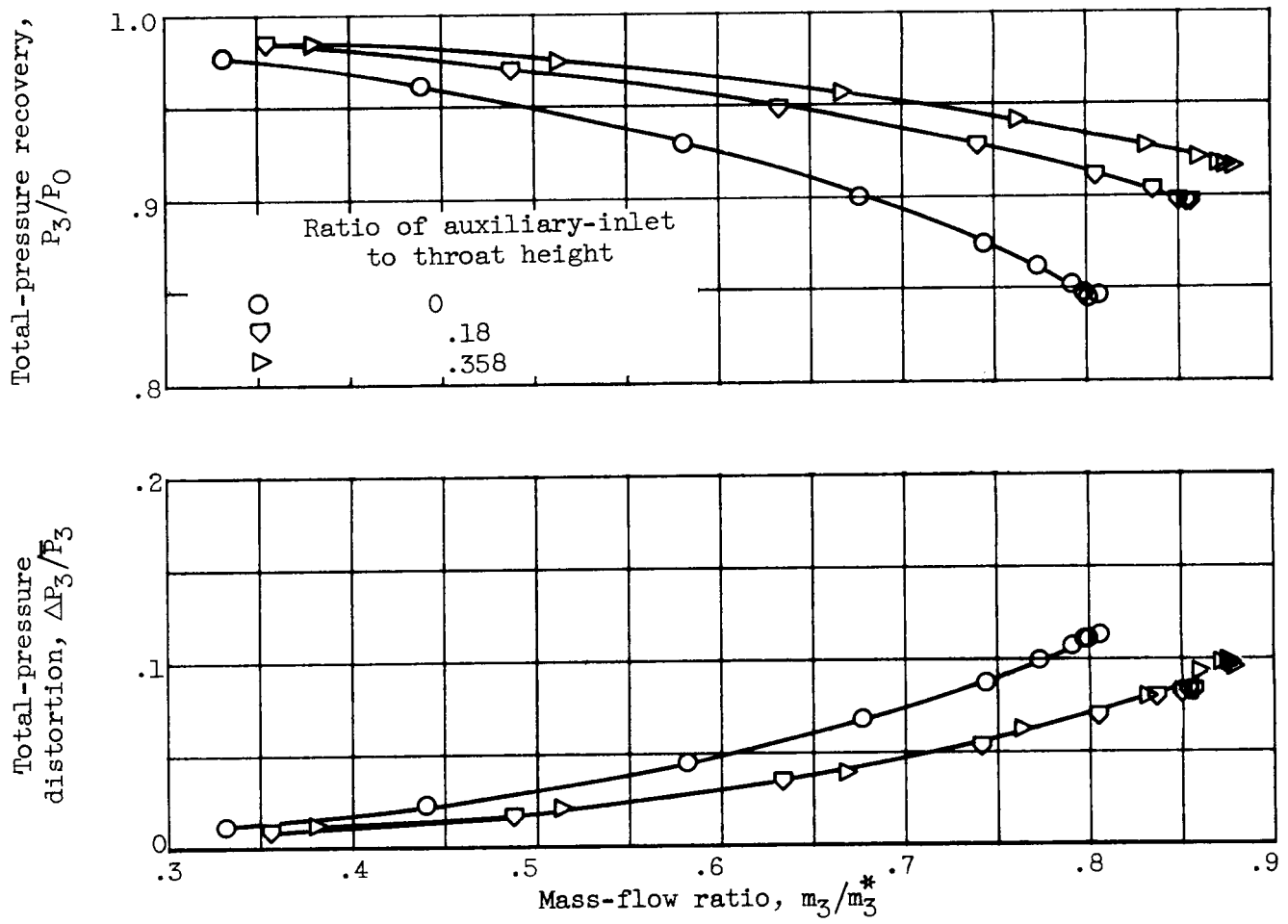

Figure 24. - Mach 0 performance of isentropic ramp with Mach 3.07 contour (-12.3° and 10.1°) with flow divider rotated into free stream and top door full open.

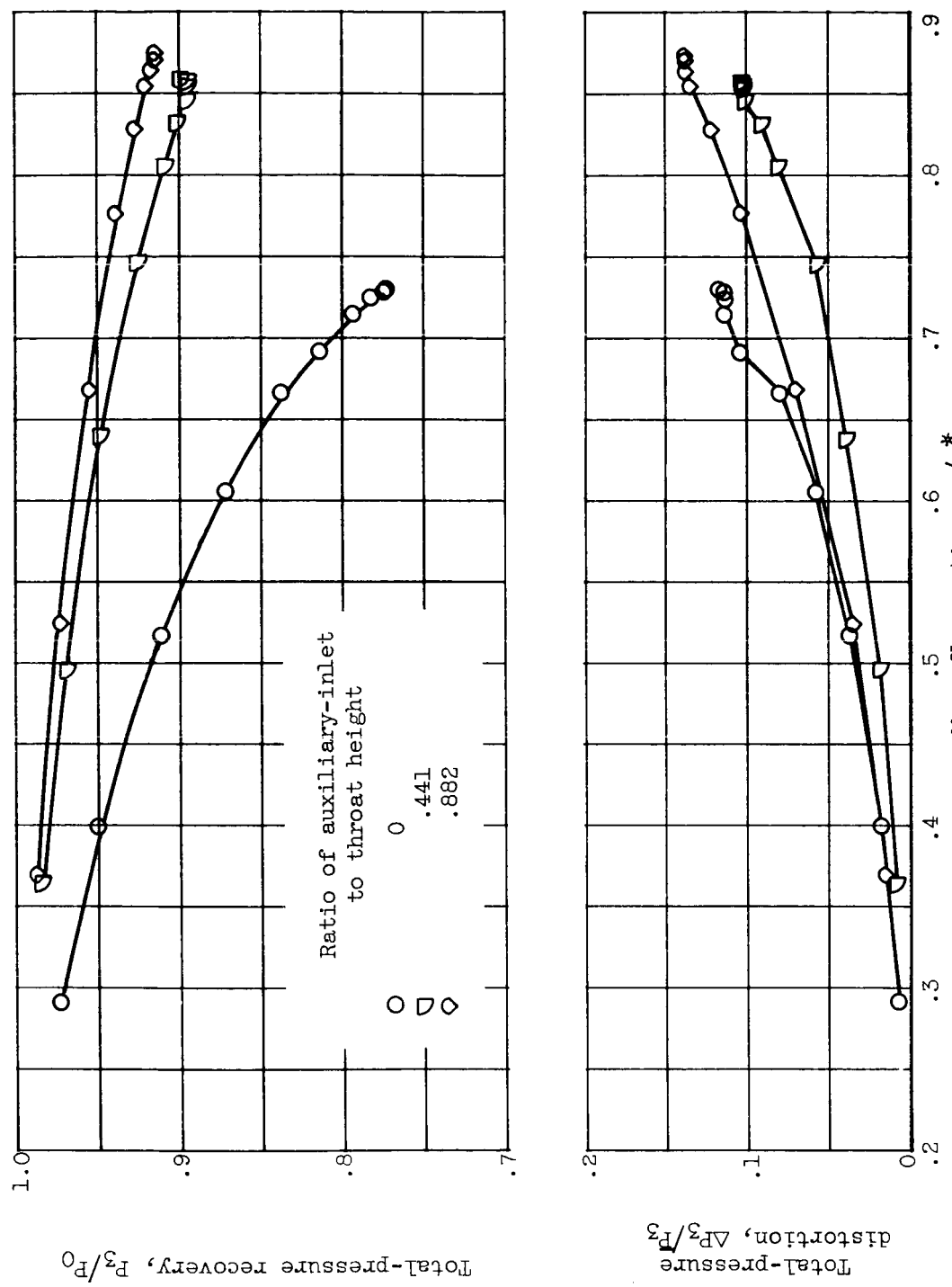

Figure 25. - Mach 0 performance of isentropic ramp with 6° flat wedge contour (6° and 6°) with flow divider rotated into free stream and top door full open.

NOTES: (1) Reynolds number is based on the diameter of a circle with the same area as that of the capture area of the inlet.

(2) The symbol * denotes the occurrence of buzz.

[redacted]

Report and facility	Description: Configuration	Description: Number of oblique shocks	Description: Type of boundary-layer control	Test parameters: Free-stream Mach number	Test parameters: Reynolds number × 10^{-6}	Test parameters: Angle of attack, deg	Test parameters: Angle of yaw, deg	Test data: Drag	Test data: Inlet-flow profile	Test data: Discharge-flow profile	Test data: Flow picture	Performance: Maximum total-pressure recovery	Performance: Mass-flow ratio	Remarks
CONFID. RM E58B13 Lewis 18- by 18-in. Mach 3.07 tunnel Lewis 18- by 18-in. Mach 1.89 tunnel Lewis duct tunnel	Two-dimensional inlet with variable external compression surfaces and various spillage methods designed for inlet-engine matching up to Mach 3. Also used with auxiliary inlet at Mach 0.	Isentropic or two oblique shocks	Throat ram scoop	3.07 1.89 0	Isentropic 0.575 2-S 0.538 Isentropic 0.97 2-S 0.907 ----------	+8 to -8	0 to 7	---- Cowl drag only ----	---- √ ----	---- √ ----	---- √ ----	0.70 0.92 ----	0.20 to 1.00	
CONFID. RM E58B13 Lewis 18- by 18-in. Mach 3.07 tunnel Lewis 18- by 18-in. Mach 1.89 tunnel Lewis duct tunnel	Two-dimensional inlet with variable external compression surfaces and various spillage methods designed for inlet-engine matching up to Mach 3. Also used with auxiliary inlet at Mach 0.	Isentropic or two oblique shocks	Throat ram scoop	3.07 1.89 0	Isentropic 0.575 2-S 0.538 Isentropic 0.97 2-S 0.907 ----------	+8 to -8	0 to 7	---- Cowl drag only ----	---- √ ----	---- √ ----	---- √ ----	0.70 0.92 ----	0.20 to 1.00	
CONFID. RM E58B13 Lewis 18- by 18-in. Mach 3.07 tunnel Lewis 18- by 18-in. Mach 1.89 tunnel Lewis duct tunnel	Two-dimensional inlet with variable external compression surfaces and various spillage methods designed for inlet-engine matching up to Mach 3. Also used with auxiliary inlet at Mach 0.	Isentropic or two oblique shocks	Throat ram scoop	3.07 1.89 0	Isentropic 0.575 2-S 0.538 Isentropic 0.97 2-S 0.907 ----------	+8 to -8	0 to 7	---- Cowl drag only ----	---- √ ----	---- √ ----	---- √ ----	0.70 0.92 ----	0.20 to 1.00	
CONFID. RM E58B13 Lewis 18- by 18-in. Mach 3.07 tunnel Lewis 18- by 18-in. Mach 1.89 tunnel Lewis duct tunnel	Two-dimensional inlet with variable external compression surfaces and various spillage methods designed for inlet-engine matching up to Mach 3. Also used with auxiliary inlet at Mach 0.	Isentropic or two oblique shocks	Throat ram scoop	3.07 1.89 0	Isentropic 0.575 2-S 0.538 Isentropic 0.97 2-S 0.907 ----------	+8 to -8	0 to 7	---- Cowl drag only ----	---- √ ----	---- √ ----	---- √ ----	0.70 0.92 ----	0.20 to 1.00	

Bibliography

These strips are provided for the convenience of the reader and can be removed from this report to compile a bibliography of NACA inlet reports. This page is being added only to inlet reports and is on a trial basis.

[redacted]